Molecular Pharmacology Fast Forward. Published on August 30, 2005 as doi:10.1124/mol.105.014795

Tweaking agonist efficacy at NMDA receptors by site-directed mutagenesis

Kasper B. Hansen, Rasmus P. Clausen, Esben J. Bjerrum, Christian Bechmann, Jeremy R. Greenwood, Caspar Christensen, Jesper L. Kristensen, Jan Egebjerg, and Hans Bräuner-Osborne.

Department of Medicinal Chemistry, Danish University of Pharmaceutical Sciences, Copenhagen, Denmark (K.B.H., R.P.C., E.J.B., C.B., J.R.G., C.C., J.L.K., H.B.-O.); Department of Molecular Neurobiology, H. Lundbeck A/S, Copenhagen, Denmark (K.B.H., C.B., J.E.).

Molecular Pharmacology Fast Forward. Published on August 30, 2005 as DOI: 10.1124/mol.105.014795
This article has not been copyedited and formatted. The final version may differ from this version.

Running Title: Tweaking agonist efficacy at NMDA receptors by mutagenesis

Corresponding Author:

Hans Bräuner-Osborne

Department of Medicinal Chemistry

Danish University of Pharmaceutical Sciences

Universitetsparken 2, DK-2100 Copenhagen, Denmark

Tel: (+45) 35 30 65 18

Fax: (+45) 35 30 60 40

Email: hbo@molpharm.net

Number of text pages: 25

Number of tables: 3

Number of figures: 12

Number of references: 29

Words in Abstract: 222

Words in Introduction: 667

Words in Discussion: 879

Abbreviations: ACBC, 1-aminocyclobutane-1-carboxylic acid; ACPC, 1-aminocyclopropane-1-carboxylic acid; AMAA, (RS)-2-amino-2-(3-hydroxy-5-methylisoxazol-4-yl)acetic acid; AMPA, 2-amino-3-(3-hydroxy-5-methylisoxazol-4-yl)propionic acid; CCG, (2S,3R,4S)-α-(carboxycyclopropyl)glycine; Cl-NHP5G, (R)-2-(4-chloro-1-hydroxy-1H-pyrazol-5-yl)glycine; HQ, homoquinolinate; NHP5G, (R)-2-(1-hydroxy-1H-pyrazol-5-yl)glycine; NMDA, N-methyl-D-aspartate.

Molecular Pharmacology Fast Forward. Published on August 30, 2005 as DOI: 10.1124/mol.105.014795
This article has not been copyedited and formatted. The final version may differ from this version.

Abstract

The structural basis for partial agonism at N-methyl-D-aspartate (NMDA) receptors is currently unresolved. We have characterized several partial agonists at the NR1/NR2B receptor and investigated the mechanisms underlying their reduced efficacy by introducing mutations in the glutamate binding site. Key residues were selected for mutation based on ligand–protein docking studies using a homology model of NR2B-S1S2 built from the X-ray structure of NR1-S1S2 in complex with glycine. Wild type and mutant forms of NR2B were co-expressed with NR1 in *Xenopus* oocytes and characterized by two-electrode voltage-clamp electrophysiology. By combining mutagenesis of residues H486 or V686 with activation by differently substituted partial agonists, we introduce varying degrees of steric clash between the ligand and the two binding domains S1 and S2. In cases where ligand–protein docking predicts increased steric clashes between agonists and the residues forming the S1-S2 interface, the agonists clearly show decreased relative efficacy. Furthermore, we demonstrate that mutating S690A affects both potency and efficacy in an agonist-specific manner. The results indicate that key residues in the ligand binding pocket of NR2B may adopt different conformations depending on the agonist bound. Altogether, these data indicates that agonist efficacy at the NR2B subunit can be controlled by the extent of steric clashes between the agonist and the ligand binding domains, and by ligand-dependent arrangements of residues within the binding pocket.

Molecular Pharmacology Fast Forward. Published on August 30, 2005 as DOI: 10.1124/mol.105.014795
This article has not been copyedited and formatted. The final version may differ from this version.

Ionotropic glutamate receptors mediate the greater proportion of fast excitatory neurotransmission in the mammalian brain, and are divided into N-methyl-D-aspartate (NMDA), 2-amino-3-(3-hydroxy-5-methylisoxazol-4-yl)propionic acid (AMPA), and kainate receptors (Dingledine et al., 1999). Whereas AMPA and kainate receptors only require binding of glutamate for activation, NMDA receptors require simultaneous binding of glycine and glutamate (Cull-Candy et al., 2001). Functional NMDA receptors typically include two NR1 subunits that bind glycine, together with two NR2 subunits possessing glutamate binding sites (Schorge and Colquhoun, 2003). The ligand binding domain of ionotropic glutamate receptor subunits is formed by two segments, S1 and S2, separated by two transmembrane domains, as well as a membrane reentrant loop which is believed to line the pore of the ion channel (Stern-Bach et al., 1994; Paas et al., 1996). Mano et al. suggested a simple clamshell model for activation and desensitization of AMPA receptors, in which the ligand binding domains S1 and S2 form an open cleft in the absence of agonist, and when an agonist binds to the cleft, the domains close around it, leading to activation of the receptor (Mano et al., 1996). X-ray structures of the ligand binding domain of the AMPA receptor GluR2 (GluR2-S1S2), alone and complexed with various agonists and antagonists, have confirmed and further refined the clamshell model (Armstrong et al., 1998; Armstrong and Gouaux, 2000; Hogner et al., 2002; Jin et al., 2003; Jin and Gouaux, 2003). In these structures there is a correlation between the degree of ligand-induced domain closure around the agonist and the extent of receptor activation. Thus antagonist binding results in little or no domain closure, and binding of full agonists gives rise to a higher degree of domain closure than does binding of partial agonists.

The glycine binding domain of the NMDA receptor subunit NR1 (NR1-S1S2) has been crystallized in complex with the full agonists glycine and D-serine, as well as the partial

agonists D-cycloserine, 1-aminocyclopropane-1-carboxylic acid (ACPC), and 1-aminocyclobutane-1-carboxylic acid (ACBC) (Furukawa and Gouaux, 2003; Inanobe et al., 2005). These X-ray structures demonstrate that like GluR2, the NR1 ligand binding cleft closes upon agonist binding. However, both full and partial agonists seem to induce the same degree of domain closure in the isolated binding domain.

Since there are presently no available X-ray structures of the glutamate binding site of NR2, several previous studies have used site-directed mutagenesis in order to identify ligand binding residues (Williams et al., 1996; Laube et al., 1997; Anson et al., 1998; Laube et al., 2004; Kalbaugh et al., 2004; Chen et al., 2005; Kinarsky et al., 2005). From these studies it can be inferred that the residues of NR2 in direct contact with glutamate share high homology with the ligand binding residues of NR1 and AMPA receptor subunits. Yet it remains uncertain what mechanisms account for partial agonism at the glutamate binding site of NR2 subunits (for review, see Erreger et al., 2004).

In the present study, we explore the mechanisms underlying partial agonism at NMDA receptors. Based on receptor modeling and ligand–protein docking we are able to introduce potential steric clashes between the ligand and residues at the interface between the two ligand binding domains (S1 and S2) of the NMDA receptor subunit NR2B. This interference is introduced in two ways: by constricting the glutamate binding site using site-directed mutagenesis and by adding steric bulk to the agonist via substituents. In this way, we demonstrate for the first time a link between agonist efficacy at NMDA receptors and the degree to which closing of the ligand binding domains (S1 and S2) is sterically hindered. Furthermore, we investigate the effect of mutating S690A on various NMDA receptor ligands, and the findings pertaining to residue S690 point to a structural basis for agonist efficacy at glutamate binding site of NR2B that involves ligand-dependent arrangements of

Molecular Pharmacology Fast Forward. Published on August 30, 2005 as DOI: 10.1124/mol.105.014795
This article has not been copyedited and formatted. The final version may differ from this version.

the residues of the binding pocket. Thus, we show data arguing that both steric hindrance of domain closure as well as ligand-dependent arrangements of the residues govern partial agonism at the binding site of NR2B.

Molecular Pharmacology Fast Forward. Published on August 30, 2005 as DOI: 10.1124/mol.105.014795
This article has not been copyedited and formatted. The final version may differ from this version.

Materials and Methods

NMDA Receptor Ligands, DNA Constructs, Site-Directed Mutagenesis. (S)-Glutamate, (2S,3R,4S)-α-(carboxycyclopropyl)glycine (CCG), N-methyl-D-aspartate (NMDA), and glycine were obtained from Sigma-Aldrich (Munich, Germany). Homoquinolinate (HQ) was obtained from Tocris (Bristol, UK). (RS)-2-amino-2-(3-hydroxy-5-methylisoxazol-4-yl)acetic acid (AMAA) was synthesized as previously described (Madsen et al., 1990). (R)-2-(1-hydroxy-1H-pyrazol-5-yl)glycine (NHP5G) and (R)-2-(4-chloro-1-hydroxy-1H-pyrazol-5-yl)glycine (Cl-NHP5G) were synthesized at the Danish University of Pharmaceutical Sciences (Copenhagen, Denmark) according to a previously published procedure (Cali and Begtrup, 2002), and resolved by chiral HPLC (to be published elsewhere).

For expression in *Xenopus* oocytes, rat NR1-1a (GenBank U11418) and rat NR2B (GenBank M91562) cDNAs were subcloned into a pCI-IRES-neo and a pCI-IRES-bla vector, respectively, containing a T7 site upstream from the 5' untranslated region. All point mutations in NR2B were introduced using a QuickChange site-directed mutagenesis kit (Stratagene, La Jolla, CA) according to the manufacturer's protocol, and verified by DNA sequencing (MWG-Biotech, Ebersberg, Germany). Constructs used for expression in *Xenopus* oocytes were linearized by restriction enzymes in order to produce cRNAs, using mMessage mMachine kits (Ambion, Huntingdon, UK).

***Xenopus* Oocyte Preparation.** Oocytes were surgically removed from mature female *Xenopus laevis* anaesthetized in a 0.4% MS-222 (3-aminobenzoic acid ethyl ester, Sigma-Aldrich) solution for 10-15 min. In order to remove the follicle layer, the oocytes were subsequently digested with 0.5 mg/ml collagenase (type IA, Sigma-Aldrich) in OR-2 buffer (in mM: 82.5 NaCl, 2.0 KCl, 1.0 $MgCl_2$, and 5.0 HEPES pH 7.6) at room temperature for 2-3 h. Healthy-looking stage V-VI oocytes were selected for injection the following day. Oocytes

Molecular Pharmacology Fast Forward. Published on August 30, 2005 as DOI: 10.1124/mol.105.014795
This article has not been copyedited and formatted. The final version may differ from this version.

were co-injected with cRNA encoding NR1-1a and NR2B at a 1:1 ratio and maintained at 18 °C in Barth´s solution (in mM: 88 NaCl, 1.0 KCl, 2.4 $NaHCO_3$, 0.41 $CaCl_2$, 0.82 $MgSO_4$, 0.3 $Ca(NO_3)_2$, and 15 HEPES pH 7.6) supplemented with 100 IU/ml penicillin and 100 μg/ml streptomycin (Invitrogen, Carlsbad, CA).

Electrophysiology. Two-electrode voltage-clamp recordings were performed 2-4 days after injection at ambient temperatures using an OC-725C Oocyte Clamp amplifier (Warner Instruments, Hampden, CT) with a Digidata 1322 interface (Axon Instruments, Union City, CA). The pClamp7 suite of programs (Axon Instruments) was used to control stimulation parameters and data acquisition. Currents were low-pass filtered at 0.01 kHz and digitized at 100 Hz. The microelectrodes were fabricated from borosilicate glass capillaries (GC150TF-10, Harvard Apparatus, Holliston, MA) and pulled on a PC-10 puller (Narishige Instruments, Tokyo, Japan). Microelectrodes were filled with 3 M KCl and had 0.5-2.5 MΩ resistance. During recording, the oocytes were voltage-clamped at –40 mV and continuously perfused with Ca^{2+}- and Mg^{2+}-free Ringer's solution containing (in mM) 115 NaCl, 2.5 KCl, 1.9 $BaCl_2$, and 10 HEPES (pH 7.6). The drugs were dissolved in Ringer's solution and applied to the oocytes by gravity-driven perfusion using a Valvebank 8 (Automate Scientific, San Francisco, CA). Due to low solubility and shift in pH of the Ringer's solution, AMAA, Cl-NHP5G, and NHP5G were applied to the oocytes at maximum concentrations of 1000 μM. Glutamate, NMDA, CCG, and HQ were used at maximum concentrations of 3000 μM. 10-20 μM glycine was included in the Ringer's solution at all times.

Data Analysis. Data was analyzed with GraphPad Prism 4.0 (GraphPad Software, San Diego, CA). Agonist concentration–response data for individual oocytes was fitted to the Hill equation: $I= I_{max}/(1+10^{((\log EC_{50}-\log[A])* n_H)})$. I_{max} is the maximum current in response to the agonist, n_H denotes the Hill coefficient, [A] is the agonist concentration, and EC_{50} is the

Molecular Pharmacology Fast Forward. Published on August 30, 2005 as DOI: 10.1124/mol.105.014795
This article has not been copyedited and formatted. The final version may differ from this version.

agonist concentration that produces half-maximum response. The EC_{50} and n_H from the individual oocytes were used to calculate the mean and standard error of mean (SEM). For graphical presentation, datasets from individual oocytes were normalized to the maximum current obtained from glutamate in the same recording, making it possible to calculate the mean and the SEM for each data point. The averaged data points were then fitted to the Hill equation and plotted together with the resulting curve. In the figures, the concentration–response fits includes the full range of the plotted concentrations, and extends the range of measured data points allowing evaluation of changes in relative maximum currents (relative I_{max}) together with changes in potencies. Relative I_{max} was calculated (unless otherwise noted) from a full concentration–response measurement as I_{max}(agonist)/I_{max}(Glu), where I_{max}(agonist) is the fitted I_{max} according to the Hill equation and I_{max}(Glu) is the maximum current obtained from glutamate in the same recording. Antagonist concentration–response data was calculated using a similar protocol, where instead of calculating the EC_{50}-value, the concentration required to inhibit a glutamate-evoked response by 50% (IC_{50}) was calculated.

Molecular Modeling and Ligand─Protein Docking. A homology model of the agonized state of NR2B was constructed as follows. The crystal structure of the soluble NR1-S1S2 construct in complex with glycine (PDB code 1PB7) (Furukawa and Gouaux, 2003) was used as a template for the ligand binding domain of NR2B. The sequence of NR2B was aligned with NR1, truncated, and the GT linker added to form a virtual NR2B-S1S2 construct containing residues 404-540 from S1 followed by the GT linker and residues 662-802 from S2. Residues are numbered according to the sequence of total wild type NR2B, including the signal peptide. NR1-S1S2 contains a loop of eight residues that is disordered and missing from the currently available crystal structures (Furukawa and Gouaux, 2003). Conveniently, NR2B has a shorter sequence of seven residues in place of this loop and the missing structural

Molecular Pharmacology Fast Forward. Published on August 30, 2005 as DOI: 10.1124/mol.105.014795
This article has not been copyedited and formatted. The final version may differ from this version.

information does not affect the quality of the homology model significantly. Given the high degree of sequence conservation between NR1 and NR2B, the construct was submitted to SWISSPROT for straightforward comparative model building with first approach mode (Schwede et al., 2000).

The GluR2-S1S2:glutamate complex (PDB code 1FTJ, chain A) (Armstrong and Gouaux, 2000) was superimposed onto the model of NR2B, and (S)-glutamate was copied from GluR2-S1S2 to NR2B-S1S2 as the endogenous tri-ionised ligand. The resulting NR2B-S1S2:glutamate complex was then used with the standard recommended refinement protocol in Impact 2.5 (pprep and impref) (Schrödinger, Portland, OR) to assign charges, add hydrogens, and perform a series of constrained minimizations, using the OPLS-AA forcefield. Van der Waals and electrostatic grids within a $(14Å + 14Å)^3$ box around the ligand position were calculated on this final model with the docking code Glide 2.5 (Schrödinger, Portland, OR); default parameters were used, apart from the scaling of non-polar atoms of the receptor that was set to 0.9. These grids were then used for ligand docking.

The ligands, NMDA, (2S,3R,4S)-α-CCG, HQ, (R)-AMAA, (R)-Cl-NHP5G, and (R)-NHP5G were submitted to Monte Carlo analysis in tri-ionised forms using the MMFFs forcefield (Halgren, 1999a; Halgren, 1999b) including GB-SA treatment of aqueous solvation in Macromodel 8.1 (Schrödinger**,** Portland, OR). The lowest energy conformations without intramolecular hydrogen bonding were flexibly docked with Glide 3.5 to the agonist binding site of the NR2B-S1S2 model. Default parameters were used, apart from the scaling factors of the radii of the non-polar receptor and ligand atoms, both set to 0.9. The mutated residues were modeled by exchanging the residues in the NR2B-S1S2:glutamate model and performing a Monte Carlo search (MMFFs forcefield) of the new side chain, while restricting the backbone of the protein and allowing flexibility of sidechains within 16 Å of the ligand.

Molecular Pharmacology Fast Forward. Published on August 30, 2005 as DOI: 10.1124/mol.105.014795
This article has not been copyedited and formatted. The final version may differ from this version.

The same procedure was used for simultaneously modeling residues T514 and S690. All figures of the models were prepared using PyMol software (DeLano Scientific, San Francisco, CA).

Molecular Pharmacology Fast Forward. Published on August 30, 2005 as DOI: 10.1124/mol.105.014795
This article has not been copyedited and formatted. The final version may differ from this version.

Results

Modeling the Glutamate Binding site of NR2B. In the absence of a high-resolution X-ray structure of the NMDA receptor glutamate binding site, we have built a homology model of the NR2B ligand binding domain based on the X-ray structure of the glycine binding domain of NR1 (Furukawa and Gouaux, 2003) (see Materials and Methods). The purpose of this model was to help direct further studies on the structural basis for potency and efficacy of NMDA receptor agonists acting at the glutamate binding site of NR2 receptor subunits. Figure 1 shows the model of the NR2B ligand binding site with glutamate copied from the GluR2 X-ray structure (1FTJ, chain A). The model can be obtained as supplemental data (See Supplemental Data).

One of the most striking differences between the NR1 and NR2B binding sites is the switch from NR1(W731) to NR2(Y731) that controls the size of the binding pocket. In NR1, W731 blocks access to the area that in NR2 binds the distal γ-carboxylate of glutamate. In our model, we identify six residues from S1 and S2 (S512, T514, R519, S690, T691, D732) that directly interact with the amino acid moiety and γ-carboxy group of glutamate via hydrogen bonds and electrostatic interactions (Fig. 1). Figure 2A outlines the numbering of residues mutated in this study and the corresponding residues in other ionotropic glutamate receptors. The α-ammonium group of glutamate is bound by the backbone carbonyl oxygen of S512 (P516 in NR1, P499 in GluR2), the side chain hydroxyl of T514, and the carboxylate oxygen of D732 (E726 in GluR2). The α-carboxy group forms a bidentate interaction with the guanidinium group of R519 and receives hydrogen bonds from the backbone amides of T514 and S690. The γ-carboxy group is positioned by interactions with the backbone amide and side chain hydroxyl of T691 (V689 in NR1). The side chain of H486 (F484 in NR1, Y471 in

Molecular Pharmacology Fast Forward. Published on August 30, 2005 as DOI: 10.1124/mol.105.014795
This article has not been copyedited and formatted. The final version may differ from this version.

GluR2) forms an electron-dense ring structure above the α- and β-carbon atoms that may function as a lid, restraining the space available and thereby facilitating binding of glutamate in the (S)-form. We speculate that the size of this aromatic residue at position 486 is linked to stereospecificity, since it faces the chiral centre of the ligand, and since NR2 generally shows a less strict preference for (S)-α-amino acids than GluR2. It is also noteworthy that H486 and V686 seem to form the entrance to a small hydrophobic pocket between the two domains (S1 and S2) in the closed conformation that allow some extra space for more bulky agonists than glutamate.

Site-Directed Mutagenesis of Residues in the NR2B Ligand Binding Pocket. In order to verify our model of the NR2B glutamate binding site, we mutated the six residues that we predict are in direct contact with glutamate (S512, T514, R519, S690, T691, D732). The effects of these mutations were tested on glutamate-evoked steady-state currents measured by two-electrode voltage-clamp recordings on *Xenopus* oocytes. In addition, the residues forming the entrance to the small pocket between S1 and S2 (H486 and V686) were also mutated. The mean EC_{50} of glutamate at these NR2B mutants are listed in Table 1, and the mean concentration–response curves are displayed in Figure 2.

T514A, R519A, T691A, and D732A mutations all give significant increases in glutamate EC_{50} (> 200-fold compared to wild type) or render the receptor non-functional (D732A), in accordance with our model that predicts that these residues form hydrogen-bonding and electrostatic interactions with glutamate via their side chains. The charge-conserving mutation R519K renders the receptor non-functional, whereas the R519A mutant retains some activity (830-fold increase in EC_{50} of glutamate) suggesting that the water architecture around the monodentate salt bridge potentially formed by lysine (R519K) is unfavorable compared to the bare water-exposed carboxylate of the ligand (R519A). Mutating residues whose backbone

Molecular Pharmacology Fast Forward. Published on August 30, 2005 as DOI: 10.1124/mol.105.014795
This article has not been copyedited and formatted. The final version may differ from this version.

atoms we predict bind to glutamate (S512A and S690A) does not have the same dramatic effect on glutamate potency. The EC_{50} of glutamate is reduced 2.7-fold by mutation S690A compared to at wild type NR2B, whereas S512A increases the EC_{50} of glutamate (33-fold). NR2B(H486L) is non-functional and the EC_{50} of glutamate increases 330-fold at NR2B(H486A) over wild type. By contrast, mutations that preserve the aromatic structure only increase the EC_{50} of glutamate 3.4-fold (H486F) and 15-fold (H486Y) demonstrating a vital role for this ring structure in coordinating agonist binding to NR2B (Table 1 and Fig. 2C).

Our model predicts that V686 does not participate in direct binding to glutamate but rather controls the size of the entrance to the small pocket between the S1 and S2 domains. Mutation of this valine to alanine or leucine would therefore not be expected to give large changes in the potency of glutamate. Accordingly, mutations V686A and V686L only increase the EC_{50} of glutamate by 7.1-fold and 3.2-fold, respectively, while mutation to the more bulky phenylalanine (V686F) increases the EC_{50} of glutamate by 20-fold relative to wild type (Table 1 and Fig. 2D).

Characterization of Partial Agonists at the NR1/NR2B Receptor. To learn more about the structural basis for potency and efficacy of partial agonists at NMDA receptors, we have characterized a number of partial agonists at NR1/NR2B. Besides the classical partial agonist NMDA, the ligands AMAA and NHP5G, recently reported to be partial agonists (Clausen *et al.*, 2004), and a novel NMDA receptor ligand Cl-NHP5G, were characterized with respect to potency and efficacy of steady-state currents relative to glutamate (Table 1 and 2, and Fig. 3). Figure 3A shows the chemical structures of all the ligands used in this study. Co-application of increasing concentrations of glutamate with each of the partial agonists demonstrated that

Molecular Pharmacology Fast Forward. Published on August 30, 2005 as DOI: 10.1124/mol.105.014795
This article has not been copyedited and formatted. The final version may differ from this version.

the reduced currents elicited by AMAA, NHP5G or Cl-NHP5G relative to glutamate are not due to secondary effects (e.g. channel block or antagonism at the glycine site) (Fig. 3D). NMDA, AMAA, NHP5G and Cl-NHP5G are all analogues of aspartate with NMDA having the highest relative agonist efficacy (0.77 ± 0.01). It is notable, that the efficacy of NHP5G (0.61 ± 0.02) relative to that of glutamate is reduced upon chloro-substitution of the heterocycle as seen with Cl-NHP5G (0.33 ± 0.01). The relative agonist efficacy of AMAA (0.58 ± 0.02) is similar to the relative efficacy of NHP5G. Both (R)-aspartate and (S)-aspartate are partial agonists at NR1/NR2B receptors with relative agonist efficacies similar to that of NMDA (Laube et al., 2004). The results also display the deleterious effect of the bulky methyl- or chloro-substituents on the potency of AMAA (EC_{50} = 47 ± 7 μM) and Cl-NHP5G (EC_{50} = 59 ± 4 μM) compared to the potency of the unsubstituted NHP5G (EC_{50} = 14 ± 1 μM).

Modeling Partial Agonist Binding in the Ligand Binding Pocket of NR2B. AMAA, Cl-NHP5G, and NHP5G were docked to the ligand binding site of the NR2B model in order to examine the structural basis for their reduced efficacy compared to glutamate. Docking initially provided several potential binding modes (known as 'poses') and in the case of AMAA, two of them corresponded to low-energy conformations. In the pose shown in Figure 4A and 4B, the heterocyclic moiety overlaps with distal carboxylic acid of glutamate. The other pose (not shown) places the amino acid moiety in the same position, but flips the heterocycle by ≈180°. Consequently, this pose was discarded due to the unlikely position of the distal acidic moiety. The novel NMDA receptor ligand Cl-NHP5G docked in the same way as AMAA, overlapping its amino acid moiety, heterocycle, and the negatively charged exocyclic oxygen. However, while the chloro-substituent of Cl-NHP5G is of similar size to

Molecular Pharmacology Fast Forward. Published on August 30, 2005 as DOI: 10.1124/mol.105.014795
This article has not been copyedited and formatted. The final version may differ from this version.

the methyl group of AMAA, it is also more spherical and the bond length to the heterocycle is longer.

Docking NHP5G gave three poses, of which one could be discarded for same reasons as above. The other two corresponded to the same conformation, with only a slight difference in the position of the amino group. The lowest energy pose is shown in Figure 4C.

Comparing the resulting binding modes of the ligands and given the order of efficacy (glutamate > NHP5G > Cl-NHP5G) (Fig. 3C), we surmise that reduced efficacy results from the steric bulk of the chloro-substituent of Cl-NHP5G or the methyl-substituent of AMAA protruding towards H486 and V686, and thus serving as a wedge between S1 and S2 (Fig. 4D).

AMAA and Cl-NHP5G are Antagonists and NHP5G is an Agonist at NR2B(H486F) and NR2B(H486Y). To evaluate how the chloro group of Cl-NHP5G and the methyl group of AMAA contribute to the observed partial agonism, we examined how the relative efficacy would be affected by increasing the size of residue H486. No currents were detected when attempting to activate NR2B(H486F) and NR2B(H486Y) with AMAA and Cl-NHP5G. However, NHP5G and NMDA were still potent agonists on these mutant NR2B subunits (Table 1 and Fig. 5). Further investigation revealed that AMAA and Cl-NHP5G are antagonists at NR2B(H486F) and NR2B(H486Y).

The relative agonist efficacies of NHP5G were reduced 2.3-fold at NR2B(H486F) and 2.9-fold at NR2B(H486Y) compared to wild type NR2B (Table 2) with small changes in agonist potencies (2.0-fold reduction (H486F) and 1.5-fold increase (H486Y) compared to the EC_{50} at wild type NR2B) (Table 1 and Fig. 5). On the other hand, the relative agonist efficacies of NMDA were only reduced 1.2-fold at NR2B(H486F) and NR2B(H486Y) compared to wild type NR2B, but the EC_{50} increased 14-fold at NR2B(H486F) and 2.2-fold at NR2B(H486Y).

Molecular Pharmacology Fast Forward. Published on August 30, 2005 as DOI: 10.1124/mol.105.014795
This article has not been copyedited and formatted. The final version may differ from this version.

In order to probe why introducing mutations H486F or H486Y selectively convert AMAA and Cl-NHP5G to antagonists while still leaving NHP5G and NMDA as agonists, we introduced these mutations to our model of the NR2B ligand binding domain. The mutations were modeled by performing a Monte Carlo search while constraining the backbone of the protein and permitting movement of side chains. In the resulting models, the mutations could be accommodated in the closed conformation of the binding domain, in agreement with the fact that glutamate still activates the mutated receptors. The lowest energy conformations of the residues were used to evaluate the steric clashes between the ligands and mutated residues.

As Figure 6 shows, the H486F mutation in S1 increases the size of the aromatic group and tilts it towards the ligands. At full domain closure there would be increased steric crowding of the chloro-substituent of Cl-NHP5G against the rim of the aromatic ring (Fig. 6A), and consequently more space in the binding pocket is needed to accommodate this ligand. AMAA, whose methyl group occupies approximately the same position as the chloro group of Cl-NHP5G, is equally affected by this mutation. NHP5G is less affected by this mutation, pointing only a hydrogen towards F486 and showing a less perpendicular arrangement between its aromatic ring and that of the phenylalanine (Fig. 6B). NMDA does not occupy the same volume in the vicinity of H486 as NHP5G, and the relative efficacy is therefore not affected to the same degree by the H486F and H486Y mutations.

Effects of Mutating V686A, V686L, and V686F on Potency and Relative Agonist Efficacy. We assessed how AMAA and Cl-NHP5G would be affected by decreases or increases in the size of residue V686 by characterizing NMDA, AMAA, Cl-NHP5G and NHP5G at NR1/NR2B(V686A), NR1/NR2B(V686L) and NR1/NR2B(V686F). None of these mutations resulted in large changes in potency for AMAA, Cl-NHP5G, or NHP5G (Table 1

Molecular Pharmacology Fast Forward. Published on August 30, 2005 as DOI: 10.1124/mol.105.014795
This article has not been copyedited and formatted. The final version may differ from this version.

and Fig. 7), but they had significant effects on the relative efficacies (Table 2 and Fig. 8). The relative efficacy of NMDA was unchanged at NR1/NR2B(V686A) and NR1/NR2B(V686L), but a decrease was observed at NR1/NR2B(V686F) (Table 2 and Fig. 8). The EC_{50} of NMDA was unaffected by V686L, but was increased 2.8-fold by V686A and 18-fold by V686F (Table 1). Reducing the size of the side chain, as in NR2B(V686A), increased the relative efficacy of NHP5G but did not affect the relative efficacies of AMAA and Cl-NHP5G. Conversely, increasing the size of the side chain, as in NR2B(V686L) and NR2B(V686F), reduced the relative efficacies for all agonists (except NMDA at NR2B(V686L)), but the reduction was much more pronounced for AMAA and Cl-NHP5G than for NHP5G or NMDA. To better illustrate this observation, Figure 8B shows the relative efficacies of NMDA, AMAA, Cl-NHP5G and NHP5G at mutant NR2B subunits as percentage of the relative efficacy at wild type NR2B. The order of the relative efficacies of all three partial agonists at wild type and mutant NR2B subunits was V686A ≥ wild type > V686L > V686F, which is also the reverse order of steric bulk introduced by the side chain of residue 686. Notably, the reduction in the relative efficacies of NMDA, AMAA, and NHP5G seems to be incremental with increasing size of the side chain of residue 686, whereas Cl-NHP5G is equally affected by V686L and V686F (Table 2 and Fig. 8).

As with H486, the mutations to V686 were modeled in order to interpret the observed reductions in relative efficacies. Mutating V686 in S2 to alanine, phenylalanine, and leucine represents differences in both size and nature of the steric bulk. Models of these mutated binding sites are shown in Figure 9. The residues are positioned so that the γ-carbons of phenylalanine and leucine overlap with the γ-carbon of valine that protrudes into the ligand binding zone. Both phenylalanine and leucine increase the volume of this intrusion by a

Molecular Pharmacology Fast Forward. Published on August 30, 2005 as DOI: 10.1124/mol.105.014795
This article has not been copyedited and formatted. The final version may differ from this version.

similar amount, however the phenyl ring presents a plane, whereas the surface of the alkyl groups is more uneven.

The chloro-substituent of Cl-NHP5G is oriented towards these residues (Fig. 9A). Thus, the spherical chloro-substituent is equally affected by phenylalanine and leucine, whereas the methyl group of AMAA seems to be affected more by phenylalanine than leucine, probably due to a better mutual fit of the grooved alkyl surfaces. NHP5G is also affected, since it points its 3-position hydrogen towards the mutated residues (Fig. 9B). However, the hydrogen is much smaller and consequently does not invoke the same steric clash as a chloro or methyl group. Thus, the efficacy of NHP5G is less affected than the efficacies of AMAA or Cl-NHP5G. NHP5G is more efficacious at NR2B(V686A) than at wild type NR2B, whereas neither the efficacy of AMAA nor Cl-NHP5G are affected by this mutation. We hypothesize that for AMAA and Cl-NHP5G, the lowered efficacy is primarily determined by the clash with H486, thus limiting an increase in efficacy at NR2B(V686A). Neither the potency nor relative efficacy of NMDA are significantly affected by V686A or V686L, but both are decreased by V686F. Substitution of V686 to phenylalanine represents a significant increase in steric bulk between S1 and S2. We speculate that upon domain closure and activation of the receptor, the phenylalanine at this position in S2 will sterically clash against residues of S1 or, in case of AMAA and Cl-NHP5G, the methyl or chloro group. This limiting of domain closure may disrupt the binding of both glutamate and NMDA and, consequently, lower their potency and efficacy at NR2B(V686F). This interpretation is further supported by the fact that the EC_{50}-values of glutamate and NMDA are affected equally by V686F (20-fold and 18-fold increases, respectively).

Ligand-Dependent Effects of Mutating S690A. The 2.7-fold decrease in the EC_{50} of glutamate observed at NR2B(S690A) (Table 1 and Fig. 2B) differs from the effect previously

Molecular Pharmacology Fast Forward. Published on August 30, 2005 as DOI: 10.1124/mol.105.014795
This article has not been copyedited and formatted. The final version may differ from this version.

described at NR2A(S689A) where a 1.7-fold increase in the EC_{50} of glutamate has been reported (Anson et al., 1998). The same serine residue has also been mutated to glycine in both NR2A (Chen et al., 2005) and NR2B (Laube et al., 1997) resulting in 120-fold and 118-fold increases in the EC_{50} of glutamate, respectively. However, glycine substitution at this position can result in altered geometry of the protein backbone, rendering the backbone amide of this residue unavailable for binding to the α-carboxy group of glutamate (Chen et al., 2005). In order to investigate the effect of the S690A mutation in more detail, we characterized two conformationally constrained analogues of glutamate, namely CCG and HQ (Fig. 3A), together with the four aspartate analogous (NMDA, AMAA, Cl-NHP5G, and NHP5G) at NR2B(S690A) (Fig. 10 and 11). The data is summarized in Table 3.

CCG is a potent agonist at wild type NR2B and S690A resulted in a slight decrease in EC_{50} (1.6-fold reduction compared to wild type NR2B), similar to the observed effect of this mutation on the EC_{50} of glutamate (2.7-fold reduction) (Fig. 2B and 10A). On the other hand, HQ and NMDA were similarly affected by S690A with 11-fold and 8.8-fold reductions in the EC_{50}-values at NR2B(S690A) compared to at wild type NR2B (Fig. 10B and C). The potencies of Cl-NHP5G, and NHP5G were largely unaffected by S690A, while the EC_{50} of AMAA was reduced 2.5-fold (Table 3 and Fig. 10).

The relative efficacies of CCG and HQ were increased 1.1-fold and 1.2-fold by the S690A mutation, respectively. In fact, the relative efficacy of all agonists increased at NR2B(S690A) compared to at wild type NR2B, with the most pronounced increases observed for AMAA (2.0-fold) and Cl-NHP5G (2.0-fold) and the smallest increase observed for CCG (Table 3 and Fig. 11).

Ligand-Induced Conformations of Residues T514 and S690. The S690A mutation mainly affected the potencies of HQ and NMDA and the efficacies of Cl-NHP5G and AMAA. To

Molecular Pharmacology Fast Forward. Published on August 30, 2005 as DOI: 10.1124/mol.105.014795
This article has not been copyedited and formatted. The final version may differ from this version.

probe the role of residue S690, ligand–protein docking of CCG, HQ, and NMDA to the ligand binding site of the NR2B model was performed (Fig. 12). Docking CCG resulted in a pose with only minor displacements in the positions of the amino acid moiety and the distal carboxy group from those of glutamate aligned according to the GluR2 X-ray structure (Fig. 12A). It is therefore not surprising to find that S690A has the same effect on CCG as glutamate. Docking HQ and NMDA resulted in poses with the α-carboxy groups overlapping with that of glutamate, the protonated nitrogens near that of glutamate, and the γ-carboxy group twisted ≈90° (Fig. 12B and C). The nitrogen of HQ only forms a single hydrogen bond to the backbone carbonyl of S512, and the α-ammonium group of NMDA only two hydrogen bonds, compared to three for glutamate. According to our model, the α-ammonium group of NMDA forms hydrogen bonds to the backbone carbonyl group of S512 and the side chain carboxylate of D732, while the N-methyl group is oriented towards T514. Consequently, T514 does not bind in the same way to glutamate as to NMDA and HQ and this residue may adopt different conformations depending on the agonist bound. Such a difference in binding can explain why the T514A mutation affects glutamate and NMDA differently; the EC_{50} of glutamate increase 200-fold at NR2B(T514A), while that of NMDA increase 38-fold (Table 1). By contrast, S512A increases the EC_{50}-values of glutamate and NMDA equally (33-fold and 34-fold, respectively). The relative I_{max} of NMDA at NR2B(S512A) and NR2B(T514A) are 0.61 ± 0.04 (N = 3) and 0.61 ± 0.01 (N = 3).

In our model, the side chain hydroxy group of S690 is close to the side chain hydroxy group of T514 when glutamate and CCG occupy the binding pocket. Changes in the conformation of T514 will therefore most likely affect the conformation of S690. The agonist-dependent conformations of T514 and S690 were modeled by performing Monte Carlo searches of these side chains with NMDA present in the binding pocket while constraining the backbone of the

Molecular Pharmacology Fast Forward. Published on August 30, 2005 as DOI: 10.1124/mol.105.014795
This article has not been copyedited and formatted. The final version may differ from this version.

protein. The results suggest that there could be alternate conformations of both T514 and S690. The lowest energy conformation in the absence of water molecules with NMDA bound is shown in Figure 12D. This conformation creates a more favorable lipophilic environment towards the N-methyl group of NMDA and the aromatic ring of HQ. However, this environment is unfavorable for ligands possessing a primary amino group (i.e. glutamate and CCG). It is notable that the ligand-dependent flipping proposed for T514 has also been observed for the corresponding T501 in GluR2 (T480 in mature GluR2) in a molecular dynamics simulation indicating a small rotation energy barrier (Arinaminpathy et al., 2002). In NR2B, the S690A mutation results in changes that are more favorable to binding of NMDA and HQ than to binding of the other agonists tested. We speculate that S690A may promote the propensity of T514 to flip, thereby increasing the potencies of NMDA and HQ significantly. In conjunction, the S690A mutation may simply create a water architecture more favorable to binding of NMDA and HQ.

Activity of AMAA, Cl-NHP5G, and NHP5G at NR2B(S690A). In the suggested binding modes of AMAA, Cl-NHP5G, and NHP5G the negatively charged exocyclic oxygen is close to the side chain hydroxy group of S690, which is unfavorable unless this hydroxy group forms a hydrogen bond to the ligands (Fig. 4). However, such a hydrogen bond is not concordant with the unaltered potencies of the agonists at NR2B(S690A) versus wild type NR2B (Table 3 and Fig. 10). In wild type NR2B, we speculate that S690 prefers to occupy the alternative flipped conformation, and instead of S690, a water molecule may be recruited to bind the exocyclic oxygen. In fact, the increased latitude of a water molecule at this position could be favorable for binding these ligands. When AMAA and Cl-NHP5G bind and activate the receptor, domain closure will result in increased steric crowding between H486 and the methyl group of AMAA or the chloro group of Cl-NHP5G pushing the exocyclic oxygen

towards this water molecule. The more flexible architecture imparted by a water molecule at this position in NR2B(S690A) would reduce the steric clashes, and we hypothesize that this is the likely explanation for the 2.0-fold increase in the relative agonist efficacies of AMAA and Cl-NHP5G observed at NR2B(S690A) (Table 3 and Fig. 11). NHP5G does not have the same potential for clashing sterically with H486 and therefore its relative agonist efficacy only increase 1.3-fold at NR2B(S690A).

The interpretation of the effects of mutation S690A prompted a closer inspection of the published NR1 structures (Furukawa and Gouaux, 2003; Inanobe et al., 2005). The suggested flipping of S690 in NR2B is also observed for the corresponding serine (S688) in the structure of NR1-S1S2 in complex with the partial agonist ACBC (Inanobe et al., 2005) (See Supplemental Data). In NR2B, it seems likely that some flexibility is present for both T514 and S690, and that the exact positions of these two residues are determined by the structure of the bound ligand and its interplay with the surrounding water architecture. In this respect, the crystal structures of NR1 presumably display the most abundant and low-energy conformational states of these residues. We suggest that agonist potency and efficacy at NR2B are tied to ligand-induced conformational changes in T514 and S690, and that the same structural features may be at work in the NR1 subunit (See Supplemental Data).

Molecular Pharmacology Fast Forward. Published on August 30, 2005 as DOI: 10.1124/mol.105.014795
This article has not been copyedited and formatted. The final version may differ from this version.

Discussion

Since the X-ray structures of the glutamate binding site of GluR2 (Armstrong et al., 1998) and glycine binding site of the NR1 subunit (Furukawa and Gouaux, 2003) were described, several studies have used these to model the glutamate binding site of NR2 (Laube et al., 2004; Chen et al., 2005; Kinarsky et al., 2005). However, since residues important for activation by glutamate were already reasonably well-defined by investigations based on sequence homology (Laube et al., 1997; Anson et al., 1998), these recent studies have mainly focused on identifying residues important for ligand discrimination. Work has also been carried out in order to determine residues important for agonist efficacy at the NR2 subunit (Laube et al., 2004; Kalbaugh et al., 2004) but none of the studies have combined homology modeling with mutational studies to address the functional effects of introducing potential steric clashes between different agonists and various residues in the binding pocket.

Steric Clashes in the Glutamate Binding Pocket of NMDA Receptors. To ensure that it is in fact potential steric clashes that are introduced between the agonist and the residues of the domain-closed binding pocket, and not some other factor that affects efficacy, it is important not to change the underlying properties of the ligand─receptor interaction. Here, histidine is changed to phenylalanine (H486F) and tyrosine (H486Y) preserving the planar ring structure; although tyrosine introduces a distal hydroxyl group, the relative efficacies of NMDA and NHP5G are similar at NR2B(H486F) and NR2B(H486Y). The hydrophobic residue valine was mutated to alanine (V686A), leucine (V686L), and phenylalanine (V686F), preserving any potential non-polar interactions in the binding pocket. Since we preserve the key interactions between the agonist and the binding site and predominately change the size of the mutated residues, we conclude that the engineered steric clashes and hence short-range

Molecular Pharmacology Fast Forward. Published on August 30, 2005 as DOI: 10.1124/mol.105.014795
This article has not been copyedited and formatted. The final version may differ from this version.

repulsive forces against the fully domain-closed binding site are responsible for the observed reduction in agonist efficacy.

Ligand-Dependent Conformations of Residues T514 and S690. The effect of mutation S690A on the EC_{50} of glutamate led to a closer examination of this residue under the influence of various ligands. These results led us to suggest that T514 and S690 will adopt different conformations depending on the agonist bound and that these ligand-induced conformations can influence potency and efficacy. Furthermore, an examination of structures of the isolated binding domain of NR1 (NR1-S1S2) suggests that similar structural features may be observed for the glycine binding site of NR1 (Furukawa and Gouaux, 2003; Inanobe et al., 2005). Functional studies at NMDA receptors have demonstrated that subsequent to agonist binding, NR1 and NR2 subunits undergo a conformational change that permits channel gating and the rate of this change is significantly slower for partial agonists than for full agonists (Banke and Traynelis, 2003). It is possible that full agonists and partial agonists induce different molecular rearrangements of residues in the binding pocket and that these different configurations could have greater or lesser probability of undergoing the conformational changes allowing channel gating on the relevant timescales. To what extent these different rearrangements also influence domain closure remains to be determined.

Mechanisms of Partial Agonism at the NR2 Subunit of NMDA Receptors. The X-ray structures of five agonist complexes of NR1 show that the full agonists glycine and D-serine cause the ligand binding domains to close to the same degree as the partial agonists D-cycloserine, ACPC, and ACBC (Furukawa and Gouaux, 2003; Inanobe et al., 2005). This finding contrasts with the link between agonist efficacy and domain closure observed for the AMPA receptor subunit GluR2. The authors suggest that partial agonists might not bind as tightly as full agonists, leading to less stabilization of the closed domains (Furukawa and

Molecular Pharmacology Fast Forward. Published on August 30, 2005 as DOI: 10.1124/mol.105.014795
This article has not been copyedited and formatted. The final version may differ from this version.

Gouaux, 2003; Inanobe et al., 2005). Current knowledge of partial agonism at NMDA receptors does not rule out the possibility that NR1 and NR2 subunits have different structural mechanisms determining agonist efficacy. In addition, different partial agonists (e.g. NMDA and AMAA) may have different structural bases for their reduced efficacy compared to glutamate. Finally, several mechanisms might be in play simultaneously to determine the efficacy of agonists at NMDA receptors.

The primary focus of this study was to address mechanisms accounting for partial agonism at the glutamate binding site of NR2 subunits. We demonstrate that the efficacies of the agonists investigated in the present study, AMAA, Cl-NHP5G, and NHP5G, are significantly reduced as a functional consequence of engineered steric clashes within the glutamate binding pocket of NR2B. Furthermore, we have used homology modeling to show that the critical steric interaction is introduced like a wedge between H486 from the S1 domain and V686 from the S2 domain. Whether the wedge prevents full closure of the ligand binding domains, or instead partially destabilizes the closed conformation, remains to be shown. However, by linking agonist efficacy to the degree to which closing of the ligand binding domains is sterically hindered, the data presented here suggest that for some agonists, partial agonism at NMDA receptors may arise from the same mechanism as at AMPA receptors, namely that the degree of receptor activation follows the degree of domain closure. Furthermore, we speculate that agonist potency and efficacy at NR2B may be influenced by ligand-dependent conformational changes of residues within the binding pocket, and that the same structural features may be present at the NR1 subunit.

Molecular Pharmacology Fast Forward. Published on August 30, 2005 as DOI: 10.1124/mol.105.014795
This article has not been copyedited and formatted. The final version may differ from this version.

Acknowledgements

The authors would like to thank Prof. Tommy Liljefors for helpful discussions and commentary on the project. We thank Dr. Ulf Madsen for generously supplying us with (RS)-AMAA. Furthermore, we acknowledge the computing resources of the Danish Center for Scientific Computing.

Molecular Pharmacology Fast Forward. Published on August 30, 2005 as DOI: 10.1124/mol.105.014795
This article has not been copyedited and formatted. The final version may differ from this version.

References

Anson LC, Chen P E, Wyllie D J, Colquhoun D and Schoepfer R (1998) Identification of Amino Acid Residues of the NR2A Subunit That Control Glutamate Potency in Recombinant NR1/NR2A NMDA Receptors. *J Neurosci* **18**:581-589.

Arinaminpathy Y, Sansom M S and Biggin P C (2002) Molecular Dynamics Simulations of the Ligand-Binding Domain of the Ionotropic Glutamate Receptor GluR2. *Biophys J* **82**:676-683.

Armstrong N and Gouaux E (2000) Mechanisms for Activation and Antagonism of an AMPA-Sensitive Glutamate Receptor: Crystal Structures of the GluR2 Ligand Binding Core. *Neuron* **28**:165-181.

Armstrong N, Sun Y, Chen G Q and Gouaux E (1998) Structure of a Glutamate-Receptor Ligand-Binding Core in Complex With Kainate. *Nature* **395**:913-917.

Banke TG and Traynelis S F (2003) Activation of NR1/NR2B NMDA Receptors. *Nat Neurosci* **6**:144-152.

Cali P and Begtrup M (2002) Synthesis of 1-Hydroxypyrazole Glycine Derivatives. *Tetrahedron* **58**:1595-1605.

Chen PE, Geballe M T, Stansfeld P J, Johnston A R, Yuan H, Jacob A L, Snyder J P, Traynelis S F and Wyllie D J (2005) Structural Features of the Glutamate Binding Site in

Recombinant NR1/NR2A N-Methyl-D-Aspartate Receptors Determined by Site-Directed Mutagenesis and Molecular Modeling. *Mol Pharmacol* **67**:1470-1484.

Clausen RP, Hansen K B, Cali P, Nielsen B, Greenwood J R, Begtrup M, Egebjerg J and Bräuner-Osborne H (2004) The Respective N-Hydroxypyrazole Analogues of the Classical Glutamate Receptor Ligands Ibotenic Acid and (RS)-2-Amino-2-(3-Hydroxy-5-Methyl-4-Isoxazolyl)Acetic Acid. *Eur J Pharmacol* **499**:35-44.

Cull-Candy S, Brickley S and Farrant M (2001) NMDA Receptor Subunits: Diversity, Development and Disease. *Curr Opin Neurobiol* **11**:327-335.

Dingledine R, Borges K, Bowie D and Traynelis S F (1999) The Glutamate Receptor Ion Channels. *Pharmacol Rev* **51**:7-61.

Erreger K, Chen P E, Wyllie D J and Traynelis S F (2004) Glutamate Receptor Gating. *Crit Rev Neurobiol* **16**:187-224.

Furukawa H and Gouaux E (2003) Mechanisms of Activation, Inhibition and Specificity: Crystal Structures of the NMDA Receptor NR1 Ligand-Binding Core. *EMBO J* **22**:2873-2885.

Halgren TA (1999a) MMFF VI. MMFF94s Option for Energy Minimization Studies. *Journal of Computational Chemistry* **20**:720-729.

Halgren TA (1999b) MMFF VII. Characterization of MMFF94, MMFF94s, and Other Widely Available Force Fields for Conformational Energies and for Intermolecular-Interaction Energies and Geometries. *Journal of Computational Chemistry* **20**:730-748.

Hogner A, Kastrup J S, Jin R, Liljefors T, Mayer M L, Egebjerg J, Larsen I K and Gouaux E (2002) Structural Basis for AMPA Receptor Activation and Ligand Selectivity: Crystal Structures of Five Agonist Complexes With the GluR2 Ligand-Binding Core. *J Mol Biol* **322**:93-109.

Inanobe A, Furukawa H and Gouaux E (2005) Mechanism of Partial Agonist Action at the NR1 Subunit of NMDA Receptors. *Neuron* **47**:71-84.

Jin R, Banke T G, Mayer M L, Traynelis S F and Gouaux E (2003) Structural Basis for Partial Agonist Action at Ionotropic Glutamate Receptors. *Nat Neurosci* **6**:803-810.

Jin R and Gouaux E (2003) Probing the Function, Conformational Plasticity, and Dimer-Dimer Contacts of the GluR2 Ligand-Binding Core: Studies of 5-Substituted Willardiines and GluR2 S1S2 in the Crystal. *Biochemistry* **42**:5201-5213.

Kalbaugh TL, VanDongen H M and VanDongen A M (2004) Ligand-Binding Residues Integrate Affinity and Efficacy in the NMDA Receptor. *Mol Pharmacol* **66**:209-219.

Kinarsky L, Feng B, Skifter D A, Morley R M, Sherman S, Jane D E and Monaghan D T (2005) Identification of Subunit- and Antagonist-Specific Amino Acid Residues in the N-

Methyl-D-Aspartate Receptor Glutamate-Binding Pocket. *J Pharmacol Exp Ther* **313**:1066-1074.

Laube B, Hirai H, Sturgess M, Betz H and Kuhse J (1997) Molecular Determinants of Agonist Discrimination by NMDA Receptor Subunits: Analysis of the Glutamate Binding Site on the NR2B Subunit. *Neuron* **18**:493-503.

Laube B, Schemm R and Betz H (2004) Molecular Determinants of Ligand Discrimination in the Glutamate-Binding Pocket of the NMDA Receptor. *Neuropharmacology* **47**:994-1007.

Madsen U, Ferkany J W, Jones B E, Ebert B, Johansen T N, Holm T and Krogsgaard-Larsen P (1990) NMDA Receptor Agonists Derived From Ibotenic Acid. Preparation, Neuroexcitation and Neurotoxicity. *Eur J Pharmacol* **189**:381-391.

Mano I, Lamed Y and Teichberg V I (1996) A Venus Flytrap Mechanism for Activation and Desensitization of Alpha-Amino-3-Hydroxy-5-Methyl-4-Isoxazole Propionic Acid Receptors. *J Biol Chem* **271**:15299-15302.

Paas Y, Eisenstein M, Medevielle F, Teichberg V I and Devillers-Thiery A (1996) Identification of the Amino Acid Subsets Accounting for the Ligand Binding Specificity of a Glutamate Receptor. *Neuron* **17**:979-990.

Schorge S and Colquhoun D (2003) Studies of NMDA Receptor Function and Stoichiometry With Truncated and Tandem Subunits. *J Neurosci* **23**:1151-1158.

Schwede T, Diemand A, Guex N and Peitsch M C (2000) Protein Structure Computing in the Genomic Era. *Res Microbiol* **151**:107-112.

Stern-Bach Y, Bettler B, Hartley M, Sheppard P O, O'Hara P J and Heinemann S F (1994) Agonist Selectivity of Glutamate Receptors Is Specified by Two Domains Structurally Related to Bacterial Amino Acid-Binding Proteins. *Neuron* **13**:1345-1357.

Williams K, Chao J, Kashiwagi K, Masuko T and Igarashi K (1996) Activation of N-Methyl-D-Aspartate Receptors by Glycine: Role of an Aspartate Residue in the M3-M4 Loop of the NR1 Subunit. *Mol Pharmacol* **50**:701-708.

Footnotes

This work was supported by the Lundbeck Foundation and the Novo Nordisk Foundation.

Reprint requests should be sent to the corresponding author Prof. Hans Bräuner-Osborne, Department of Medicinal Chemistry, Danish University of Pharmaceutical Sciences, Universitetsparken 2, DK-2100 Copenhagen, Denmark.

Molecular Pharmacology Fast Forward. Published on August 30, 2005 as DOI: 10.1124/mol.105.014795
This article has not been copyedited and formatted. The final version may differ from this version.

Figure Legends

Figure 1. Key interactions between glutamate and residues in the glutamate binding pocket of NR2B. The homology model of the glutamate binding site of NR2B was built using the glycine binding site of NR1 as a template. The GluR2-S1S2:glutamate complex (PDB code 1FTJ, chain A) was superimposed onto the model of NR2B, and glutamate was copied from GluR2-S1S2 to NR2B-S1S2 as the endogenous ligand. Glutamate binds via hydrogen bonds and electrostatic interactions (green dotted lines) to three residues from S1 (S512, T514, R519) and three residues from S2 (S690, T691, D732). Y731 (W731 in NR1) controls whether there is access to the distal γ-carboxylate binding zone, and thus whether glycine or glutamate binds to the receptor. H486 and V686 form the entrance to a small hydrophobic pocket between the two domains (S1 and S2) in the closed conformation. Carbon (grey), nitrogen (blue), oxygen (red), and hydrogen (white) atoms of the binding pocket are presented as sticks and atoms of glutamate are presented as ball and stick. A, the binding pocket viewed from an angle through H486 and V686. B, the binding pocket viewed from a different angle through Y731. The model can be obtained as supplemental data (See Supplemental Data).

Figure 2. A, NR2B residues mutated in this study (listed in bold) and their corresponding positions in NR2A, NR1, and GluR2. In this study, residues are numbered with respect to the amino acid sequence of the total protein including the signal peptide. Since some studies number residues with respect to the amino acid sequence of the mature protein without the predicted signal peptide these numbers are also listed here for reference. B, mean concentration–response curves for glutamate at NR1/NR2B(S690A) (●), wild type NR1/NR2B (■), NR1/NR2B(S512A) (◊), NR1/NR2B(T514A) (○), NR1/NR2B(T691A) (▼), and NR1/NR2B(R519A) (♦). C, mean concentration–response curves for glutamate at wild

type NR1/NR2B (■), NR1/NR2B(H486A) (●), NR1/NR2B(H486F) (▲), and NR1/NR2B(H486Y) (▼). D, mean concentration–response curves for glutamate at NR1/NR2B receptors with wild type (■), V686A (●), V686L (▲), and V686F (▼) NR2B subunits. The EC_{50}-values and Hill coefficients are listed in Table 1.

Figure 3. A, chemical structures of the NMDA receptor ligands characterized at wild type and mutant NR1/NR2B receptors in this study. B, mean concentration–response curves for AMAA (■), Cl-NHP5G (●), NHP5G (▲), and NMDA (▼) at the NR1/NR2B receptor. The curves are normalized to the I_{max} of glutamate. The EC_{50}-values and Hill coefficients are listed in Table 1. C, relative efficacies for the four partial agonists AMAA, Cl-NHP5G, NHP5G, and NMDA at the NR1/NR2B receptor, shown here as the I_{max} of the agonist relative to the I_{max} obtained from glutamate in the same recording. The steady-state I_{max} was measured by two-electrode voltage-clamp recordings on *Xenopus* oocytes. The values are listed in Table 2. D, normalized currents evoked by AMAA (white), Cl-NHP5G (black), and NHP5G (grey) at the NR1/NR2B receptor either alone or together with 30 μM or 300 μM glutamate. Currents are normalized to the response evoked by 300 μM glutamate alone.

Figure 4. Ligand-protein docking of AMAA, Cl-NHP5G, and NHP5G into the ligand binding pocket of NR2B. Carbon (grey), nitrogen (blue), oxygen (red), and hydrogen (white) atoms of the binding pocket are presented as sticks and atoms of the ligands as ball and stick. Carbon atoms of glutamate (orange), AMAA (salmon), Cl-NHP5G (cyan), and NHP5G (marine) are presented in different colors. A, binding of AMAA and glutamate viewed perpendicular to H486 and V686. Y731 is omitted for clarity. B, binding of AMAA and glutamate viewed from an angle through H486 and V686. The methyl-substituent protrudes directly towards the space between H486 and V686. C, binding of NHP5G and glutamate viewed perpendicular to H486 and V686. Y731 is omitted for clarity. D, binding of Cl-NHP5G, which binds similarly

Molecular Pharmacology Fast Forward. Published on August 30, 2005 as DOI: 10.1124/mol.105.014795
This article has not been copyedited and formatted. The final version may differ from this version.

to AMAA, shown with NR2B-S1S2 presented in ribbon, in order to illustrate that the chloro-substituent (pink) of Cl-NHP5G protrudes towards H486 and V686, acting like a wedge between S1 (blue) and S2 (red).

Figure 5. A, mean concentration–response curves for NMDA at wild type NR1/NR2B (■), NR1/NR2B(H486F) (●), and NR1/NR2B(H486Y) (▲). B, mean concentration–response curves for NHP5G. The curves are normalized to the I_{max} of glutamate at the same NR2B subunit. C, mean concentration–response curves for inhibition of currents evoked by 30 μM glutamate by AMAA (■) and Cl-NHP5G (●) at NR1/NR2B(H486F) receptors. D, mean concentration–response curves for inhibition of currents evoked by 10 μM glutamate by AMAA (■) and Cl-NHP5G (●) at NR1/NR2B(H486Y) receptors. E, representative responses obtained from a two-electrode voltage-clamp recording on a *Xenopus* oocyte expressing the mutant NR1/NR2B(H486Y) receptor. Currents were evoked by co-application of 10 μM glutamate and Cl-NHP5G (in the presence of 10 μM glycine) at the concentration indicated above each response.

Figure 6. Modeling of the H486F mutation in the NR2B ligand binding pocket. The H486F mutation in S1 increases the size of the aromatic group and tilts it towards the ligands. Carbon (grey), nitrogen (blue), and oxygen (red) atoms of the binding pocket are presented as sticks and atoms of the ligands, H486, and F486 as ball and stick. Carbon atoms of glutamate are presented in orange. Y731 and hydrogen atoms are omitted for clarity. A, binding of Cl-NHP5G viewed perpendicular to H486 and V686. The chloro-substituent (pink) protrudes directly towards the space between H486 and V686. B, binding of NHP5G viewed from the same angle.

Figure 7. A, mean concentration–response curves for NMDA. B, mean concentration–response curves for NHP5G. C, mean concentration–response curves for AMAA. D, mean

Molecular Pharmacology Fast Forward. Published on August 30, 2005 as DOI: 10.1124/mol.105.014795
This article has not been copyedited and formatted. The final version may differ from this version.

concentration–response curves for Cl-NHP5G. All curves are normalized to the I_{max} of glutamate at the same NR2B subunit. The EC_{50}-values and hill coefficients are listed in Table 1. E, representative maximum currents evoked by Cl-NHP5G and glutamate at wild type NR1/NR2B (left) or mutant NR1/NR2B(V686F) (right).

Figure 8. A, relative efficacies for the four partial agonists AMAA (white), Cl-NHP5G (black), NHP5G (grey), and NMDA (striped) at NR1/NR2B receptors with V686A, wild type, V686L, and V686F NR2B subunits, shown here as the I_{max} of the agonist relative to the I_{max} obtained from glutamate in the same recording. The values are listed in Table 2. B, the same data as in A displayed as percentage of the relative I_{max} of the same agonist at wild type NR1/NR2B in order to better visualize the more pronounced reduction in the relative efficacies of AMAA (white) and Cl-NHP5G (black) compared to NHP5G (grey) and NMDA (striped).

Figure 9. Modeling of the V686A, V686L, and V686F mutations in the NR2B ligand binding pocket. The residues are positioned so that the γ-carbons of phenylalanine and leucine overlap with the γ-carbon of valine that protrudes into the ligand binding zone. Both phenylalanine and leucine increase this intrusion by a similar amount, but the phenyl ring presents a flat surface whereas the alkyl group is more uneven. The β-carbon of alanine overlaps with that of valine and is therefore omitted for clarity. Carbon (grey), nitrogen (blue), and oxygen (red) atoms of the binding pocket are presented as sticks and atoms of the ligands, V686, L686, and F686 as ball and stick. Carbon atoms of glutamate are presented in orange. Y731 and hydrogen atoms are omitted for clarity. A, binding of Cl-NHP5G viewed perpendicular to H486 and V686. The chloro-substituent (pink) protrudes directly towards the space between H486 and V686. B, binding of NHP5G viewed from the same angle.

Molecular Pharmacology Fast Forward. Published on August 30, 2005 as DOI: 10.1124/mol.105.014795
This article has not been copyedited and formatted. The final version may differ from this version.

Figure 10. Mean concentration–response curves for CCG (A), HQ (B), NMDA (C), NHP5G (D), Cl-NHP5G (E), and AMAA (F) at wild type NR1/NR2B (□) and mutant NR1/NR2B (S690A) (■). All curves are normalized to the I_{max} of glutamate at the same NR2B subunit. The parameters are summarized in Table 3.

Figure 11. A, relative efficacies for AMAA, Cl-NHP5G, NHP5G, NMDA, CCG, and HQ at wild type NR1/NR2B (white) and mutant NR1/NR2B (S690A) (black) shown here as the I_{max} of the agonist relative to the I_{max} obtained from glutamate in the same recording. B, the same data as in A displayed as percentage of the relative I_{max} of the same agonist at wild type NR1/NR2B. The parameters are summarized in Table 3.

Figure 12. Ligand–protein docking of CCG, HQ, and NMDA into the ligand binding pocket of NR2B. Carbon (grey), nitrogen (blue), and oxygen (red) atoms of the binding pocket are presented as sticks and atoms of the ligands as ball and stick. Carbon atoms of glutamate are presented in orange and carbon atoms of CCG, HQ, and NMDA are presented in marine. All hydrogen atoms are omitted for clarity. Hydrogen bonds between glutamate and residues of the binding pocket are shown as green dotted lines. A, binding of CCG and glutamate. B, binding of HQ and glutamate. C, binding of NMDA and glutamate. D, binding of NMDA and glutamate with T514 and S690 flipped and the hydrogen bond from the side chain of T514 to glutamate removed. Carbon atoms of the flipped T514 and S690 side chains are presented in green.

Molecular Pharmacology Fast Forward. Published on August 30, 2005 as DOI: 10.1124/mol.105.014795
This article has not been copyedited and formatted. The final version may differ from this version.

Table 1. Potency of agonists at the NR1/NR2B receptor with wild type or mutant NR2B subunits.

	Glutamate		NMDA		AMAA		Cl-NHP5G		NHP5G	
NR2B mutant	EC_{50} (μM) (n_H)	N	EC_{50} (μM) (n_H)	N	EC_{50} (μM) (n_H)	N	EC_{50} (μM) (n_H)	N	EC_{50} (μM) (n_H)	N
WT	1.6 ± 0.1 (1.7)	4	22 ± 2 (1.4)	7	47 ± 6 (1.5)	6	59 ± 4 (1.2)	6	14 ± 1 (1.4)	4
H486A	520 ± 90 (1.4)	5	> 1000		NR		NR		NR	
H486F	5.5 ± 0.9 (1.6)	7	310 ± 20 (1.5)	5	[8.3 ± 0.3 (0.9)]	7	[130 ± 10 (0.8)]	6	7.1 ± 0.3 (1.0)	3
H486L	NR		ND		NR		NR		ND	
H486Y	24 ± 1 (1.4)	6	48 ± 1 (1.6)	4	[7.9 ± 0.2 (1.1)]	7	[38 ± 1 (1.0)]	6	21 ± 4 (1.2)	3
S512A	52 ± 5 (1.4)	5	760 ± 30 (2.0)	3	ND		ND		ND	
T514A	320 ± 20 (1.3)	5	620 ± 20 (2.0)	3	ND		ND		ND	
R519A	1300 ± 200 (1.5)	4	ND		ND		ND		ND	
R519K	NR		ND		ND		ND		ND	
V686A	11 ± 1 (1.6)	5	61 ± 3 (1.6)	5	52 ± 7 (1.2)	4	110 ± 10 (1.1)	6	22 ± 1 (1.2)	5
V686F	31 ± 3 (1.4)	5	400 ± 11 (1.6)	5	61 ± 9 (1.3)	5	140 ± 30 (1.3)	3	51 ± 9 (1.3)	4
V686L	5.1 ± 0.2 (1.5)	4	16 ± 1 (1.4)	5	87 ± 12 (1.1)	5	88 ± 19 (1.2)	4	41 ± 2 (1.7)	5
S690A	0.6 ± 0.1 (1.3)	6	2.5 ± 0.2 (1.5)	4	19 ± 1 (1.2)	5	72 ± 10 (1.5)	4	21 ± 1 (1.8)	5
T691A	840 ± 40 (1.7)	3	> 3000		NR		NR		NR	
D732A	NR		ND		ND		ND		ND	

Parameters measured from steady-state currents by two-electrode voltage-clamp recordings on *Xenopus* oocytes. Mean EC_{50} ± SEM was calculated from concentration–response measurements and the mean respective Hill coefficients (n_H) are given in parentheses. N denotes the number of oocytes. IC_{50}-values for inhibition of currents evoked by 30 μM glutamate at NR2B(H486F) and by 10 μM glutamate at NR2B(H486Y) are shown in brackets. NR, no response to 1000 μM of the agonist. ND, not determined.

Molecular Pharmacology Fast Forward. Published on August 30, 2005 as DOI: 10.1124/mol.105.014795
This article has not been copyedited and formatted. The final version may differ from this version.

Table 2. Relative efficacies of partial agonists at the NR1/NR2B receptor with wild type or mutant NR2B subunits.

	NMDA	AMAA	Cl-NHP5G	NHP5G
NR2B mutant	Relative I_{max} (N)	Relative I_{max} (N)	Relative I_{max} (N)	Relative I_{max} (N)
WT	0.77 ± 0.01 (4)	0.58 ± 0.02 (32)	0.33 ± 0.01 (6)	0.61 ± 0.02 (4)
H486F	0.64 ± 0.02 (5) *	Antagonist	Antagonist	0.27 ± 0.02 (3) *
H486Y	0.63 ± 0.01 (4) *	Antagonist	Antagonist	0.21 ± 0.03 (3) *
V686A	0.75 ± 0.03 (5)	0.58 ± 0.03 (4)	0.35 ± 0.02 (6)	0.72 ± 0.01 (5) *
V686F	0.57 ± 0.01 (5) *	0.04 ± 0.01 (5) *	0.04 ± 0.01 (3) *	0.31 ± 0.02 (4) *
V686L	0.73 ± 0.02 (5)	0.25 ± 0.02 (9) *	0.08 ± 0.01 (4) *	0.39 ± 0.05 (6) *
S690A	0.93 ± 0.02 (4) *	1.15 ± 0.03 (28) *	0.67 ± 0.05 (4) *	0.78 ± 0.02 (5) *

Maximum steady-state currents (I_{max}) was measured by two-electrode voltage-clamp recordings on *Xenopus* oocytes. Relative I_{max} were calculated from a full concentration–response measurement as the fitted I_{max} according to the Hill equation divided by I_{max} obtained from glutamate in the same recording. Mean relative I_{max} is listed ± SEM. The number in parentheses (N) denotes the number of oocytes. Unpaired Student's t-test was used for comparison of the relative I_{max} of a given agonist at mutant NR2B with the relative I_{max} of the same agonist at wild type NR2B. * $p<0.05$.

Molecular Pharmacology Fast Forward. Published on August 30, 2005 as DOI: 10.1124/mol.105.014795
This article has not been copyedited and formatted. The final version may differ from this version.

Table 3. Potency and relative efficacy of agonists at wild type NR1/NR2B and mutant NR1/NR2B(S690A).

	NR1/NR2B			NR1/NR2B(S690A)		
Agonist	EC_{50} (μM) (N)	n_H	Relative I_{max} (N)	EC_{50} (μM) (N)	n_H	Relative I_{max} (N)
Glutamate	1.6 ± 0.1 (4)	1.7	-	0.6 ± 0.1 (6)	1.3	-
CCG	0.055 ± 0.002 (9)	1.7	1.08 ± 0.02 (9)	0.034 ± 0.001 (5)	1.9	1.18 ± 0.01 (5)
HQ	21 ± 2 (9)	1.5	1.04 ± 0.02 (9)	2.0 ± 0.1 (6)	1.3	1.28 ± 0.01 (6)
NMDA	22 ± 2 (7)	1.4	0.77 ± 0.01 (4)	2.5 ± 0.2 (4)	1.5	0.93 ± 0.02 (4)
NHP5G	14 ± 1 (4)	1.4	0.61 ± 0.02 (4)	21 ± 1 (5)	1.8	0.78 ± 0.02 (5)
Cl-NHP5G	59 ± 4 (6)	1.2	0.33 ± 0.01 (6)	72 ± 10 (4)	1.5	0.67 ± 0.05 (4)
AMAA	47 ± 6 (6)	1.5	0.58 ± 0.02 (32)	19 ± 1 (5)	1.2	1.15 ± 0.03 (28)

Parameters measured from steady-state currents by two-electrode voltage-clamp recordings on *Xenopus* oocytes. Mean EC_{50} ± SEM, mean respective Hill coefficients (n_H), and mean relative I_{max} ± SEM are calculated as in Table 1 and 2. The number in parentheses (N) denotes the number of oocytes.

Figure 1

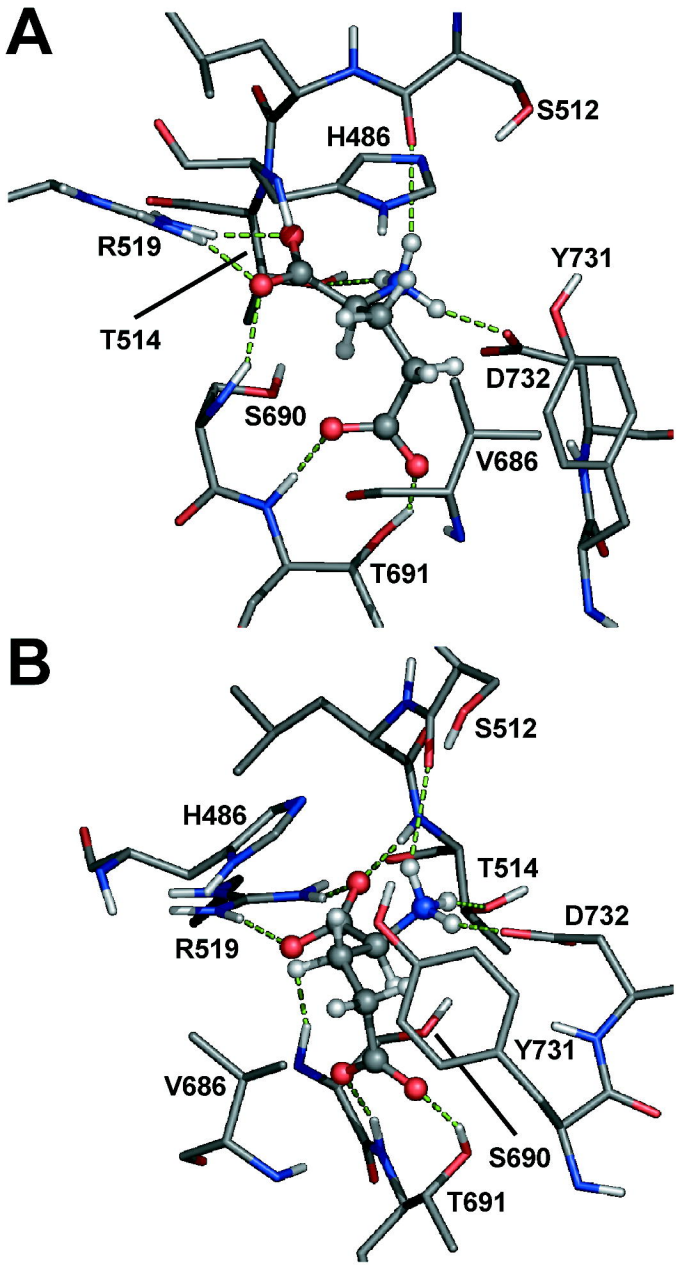
A
S512
H486
R519
Y731
T514
D732
S690
V686
T691
B
S512
H486
T514
D732
R519
Y731
V686
S690
T691

Figure 2

A

Total protein				Mature protein			
NR2B	**NR2A**	**NR1**	**GluR2**	**NR2B**	**NR2A**	**NR1**	**GluR2**
H486	H485	F484	Y471	H460	H466	F466	Y450
S512	S511	P516	P499	S486	S492	P498	P478
T514	T513	T518	T501	T488	T494	T500	T480
R519	R518	R523	R506	R493	R499	R505	R485
V686	V685	V684	L671	V660	V666	V666	L650
S690	S689	S688	S675	S664	S670	S670	S654
T691	T690	V689	T676	T665	T671	V671	T655
D732	D731	D732	E726	D706	D712	D714	E705

B

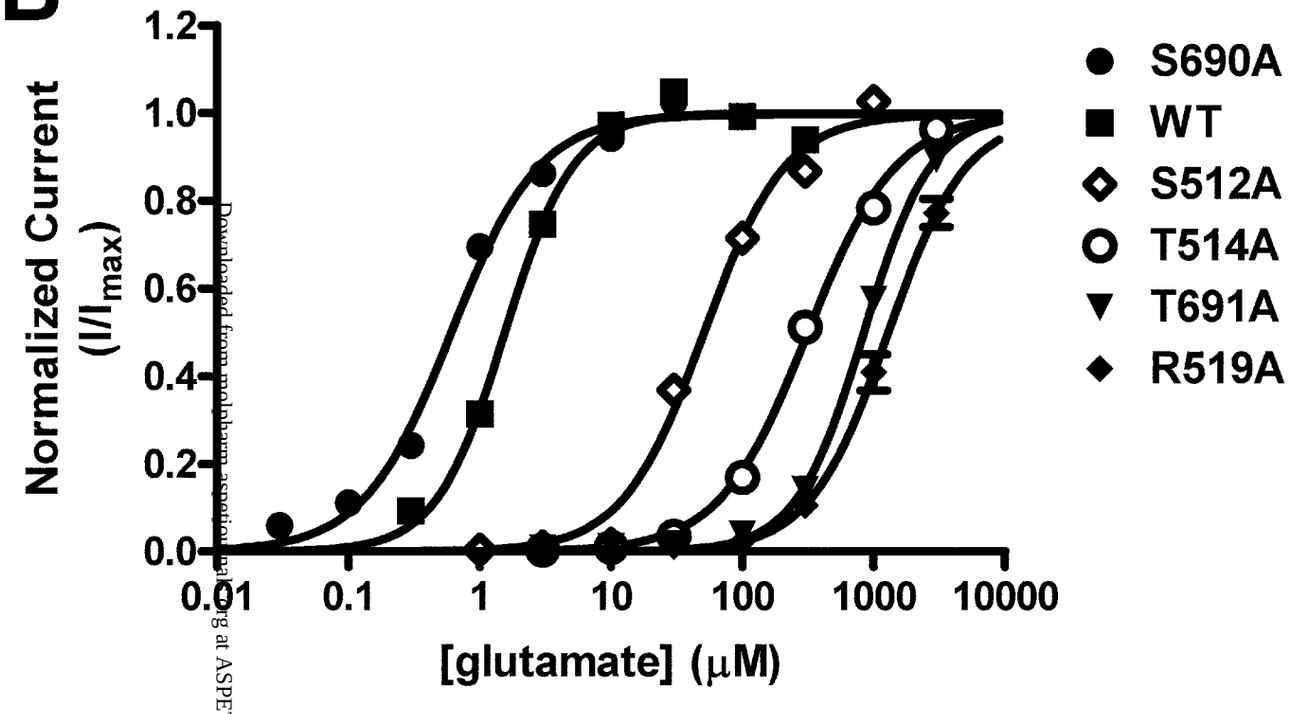

C

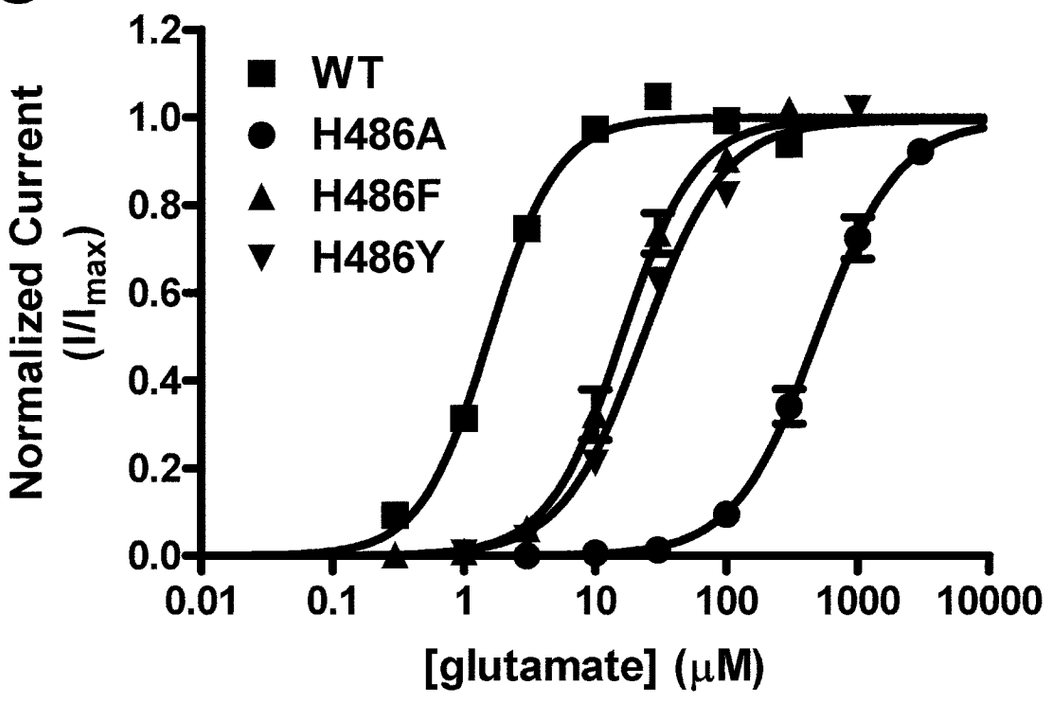

D

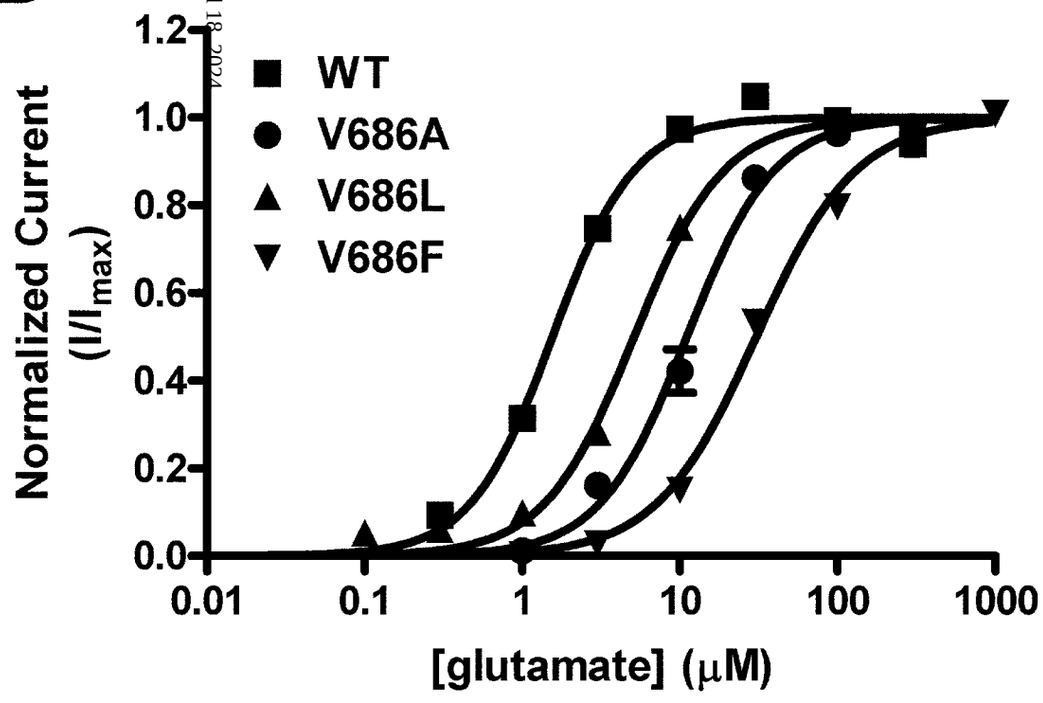

Figure 3

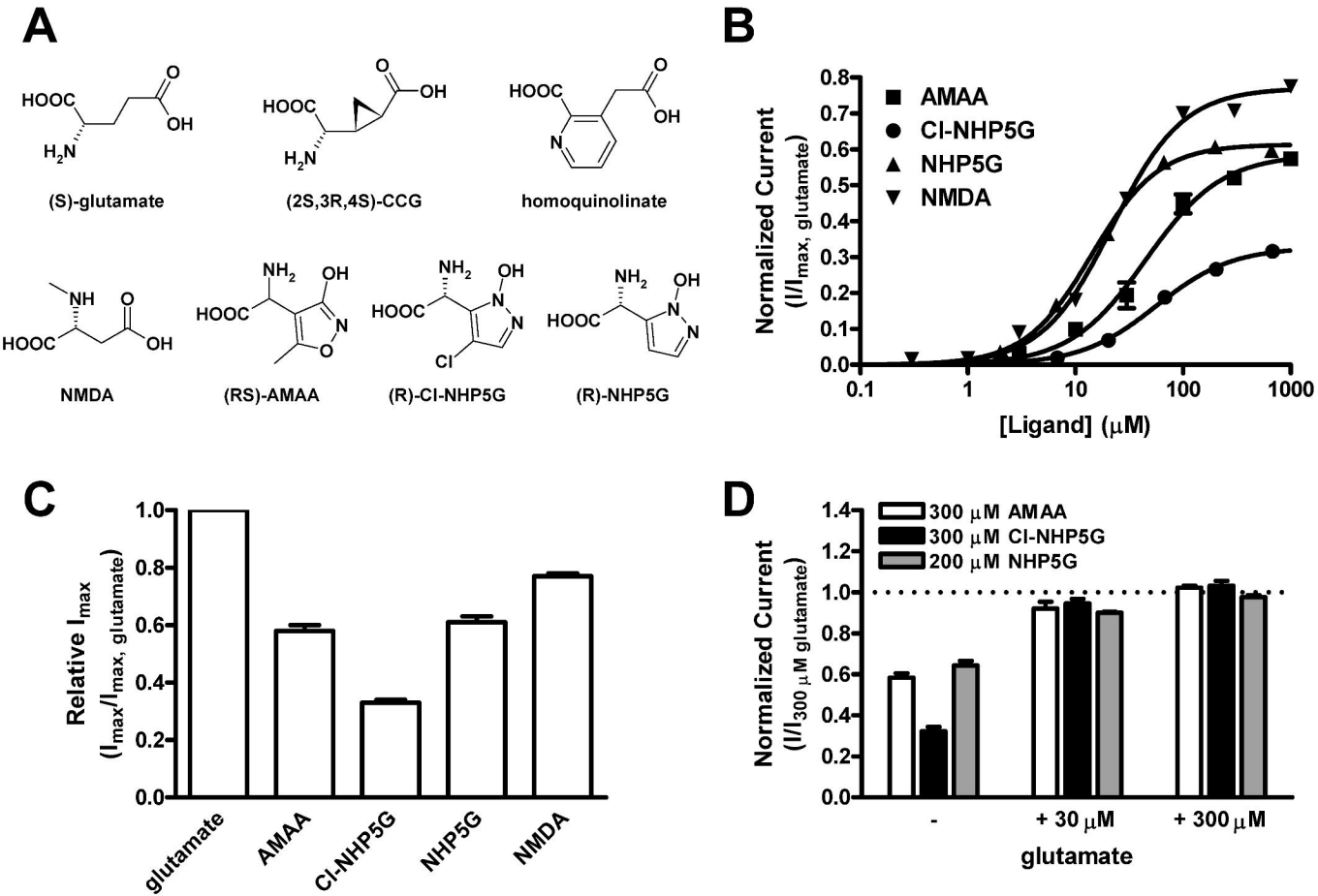
A
(S)-glutamate
(2S,3R,4S)-CCG
homoquinolinate
NMDA
(RS)-AMAA
(R)-Cl-NHP5G
(R)-NHP5G
B
AMAA
Cl-NHP5G
NHP5G
NMDA
Normalized Current
(I/Imax, glutamate)
[Ligand] (μM)
C
Relative Imax
(Imax/Imax, glutamate)
glutamate
AMAA
Cl-NHP5G
NHP5G
NMDA
D
300 μM AMAA
300 μM Cl-NHP5G
200 μM NHP5G
Normalized Current
(I/I300 μM glutamate)
-
+ 30 μM
+ 300 μM
glutamate

Figure 4

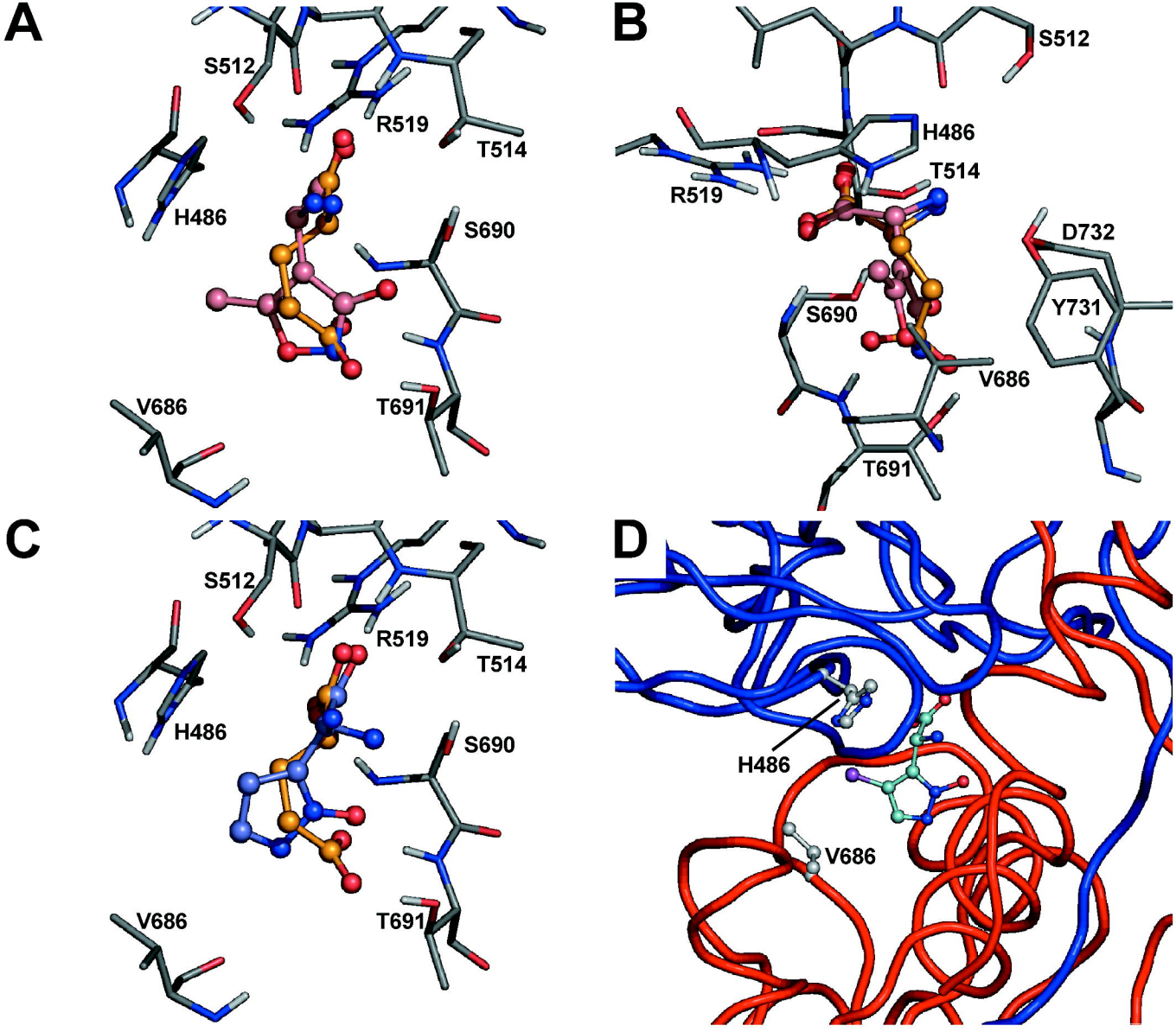
A
S512
R519
T514
H486
S690
V686
T691
B
S512
H486
T514
R519
D732
Y731
S690
V686
T691
C
S512
R519
T514
H486
S690
V686
T691
D
H486
V686

Figure 5

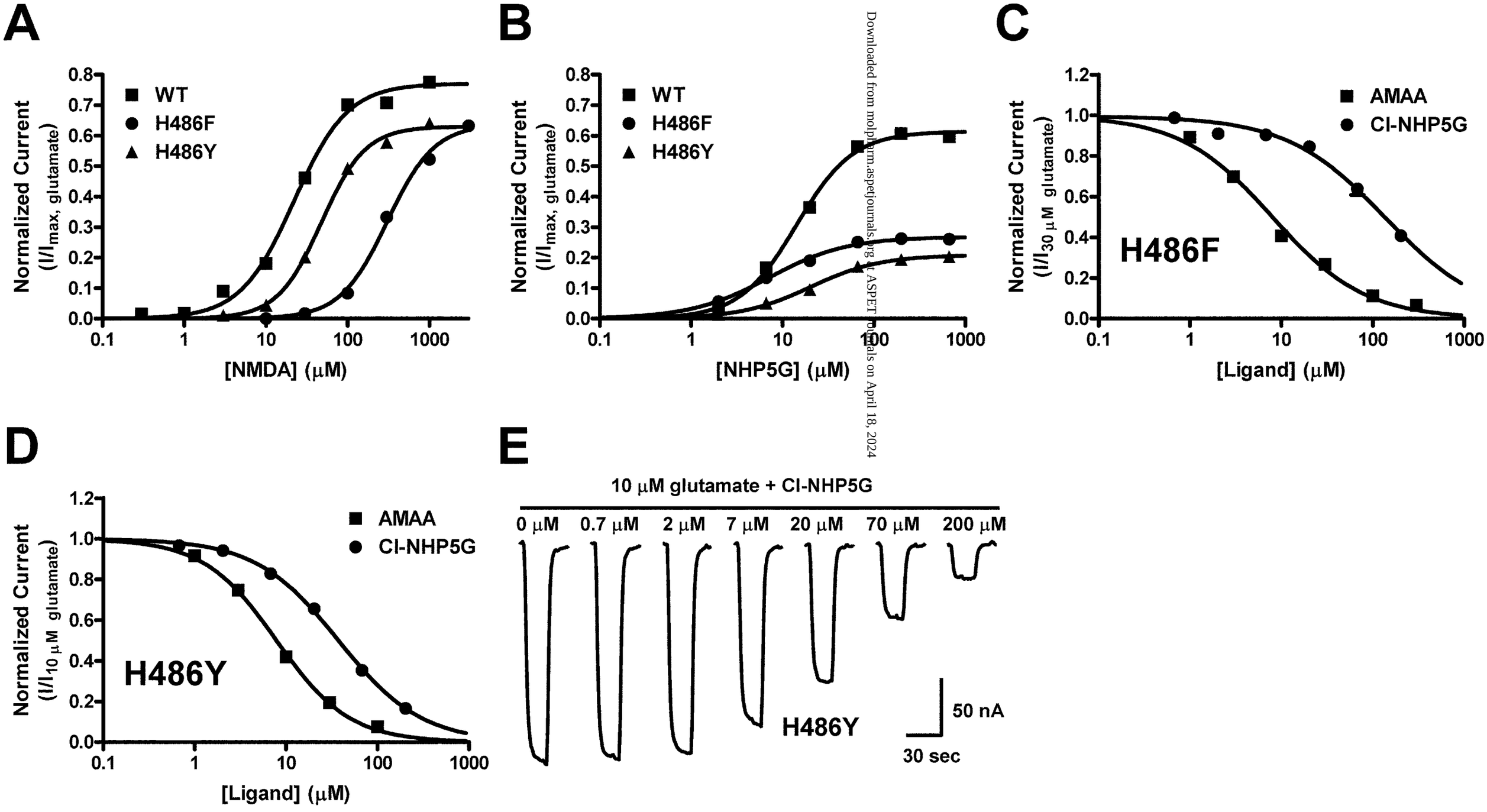

Figure 6

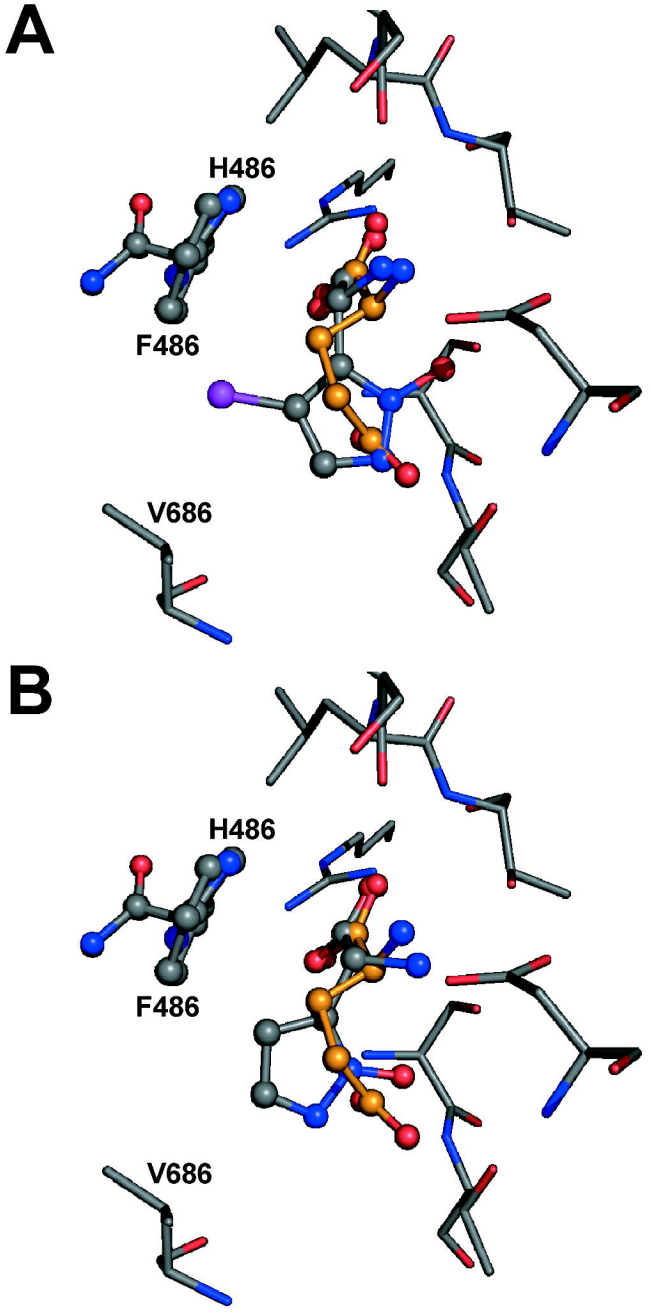

Figure 7

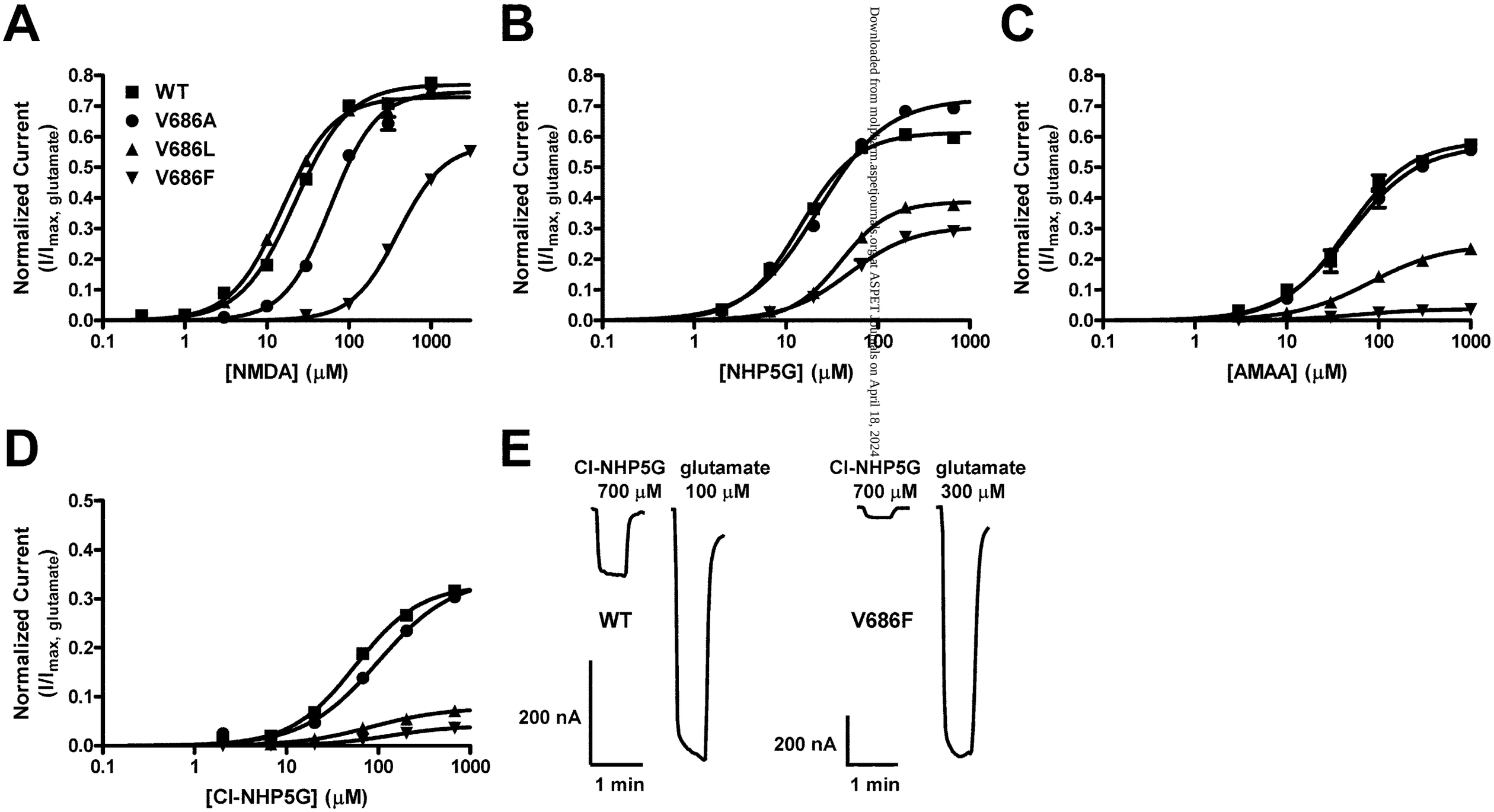

Figure 8

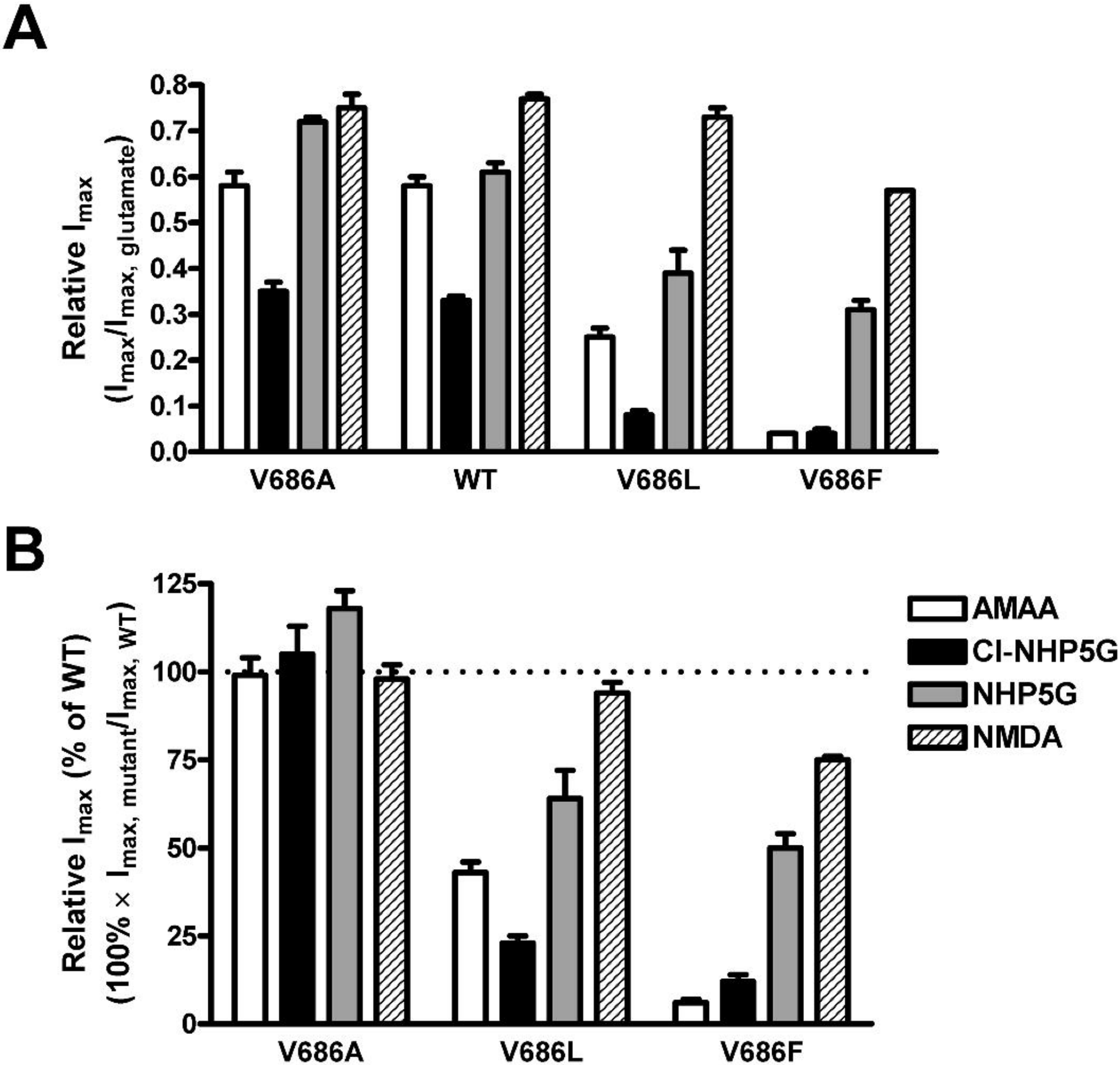
A
Relative I_{max}
($I_{max}/I_{max, glutamate}$)
0.8
0.7
0.6
0.5
0.4
0.3
0.2
0.1
0.0
V686A
WT
V686L
V686F
B
Relative I_{max} (% of WT)
($100\% \times I_{max, mutant}/I_{max, WT}$)
125
100
75
50
25
0
V686A
V686L
V686F
AMAA
CI-NHP5G
NHP5G
NMDA

Figure 9

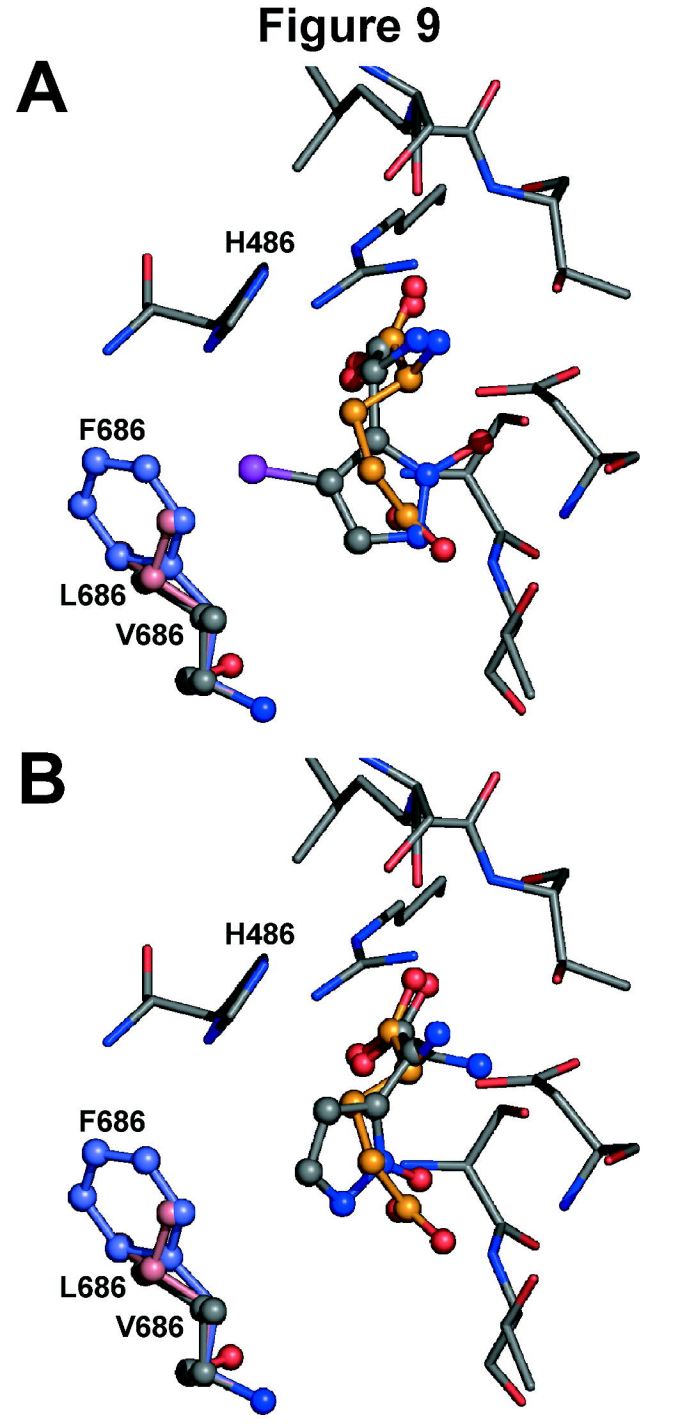

Figure 10

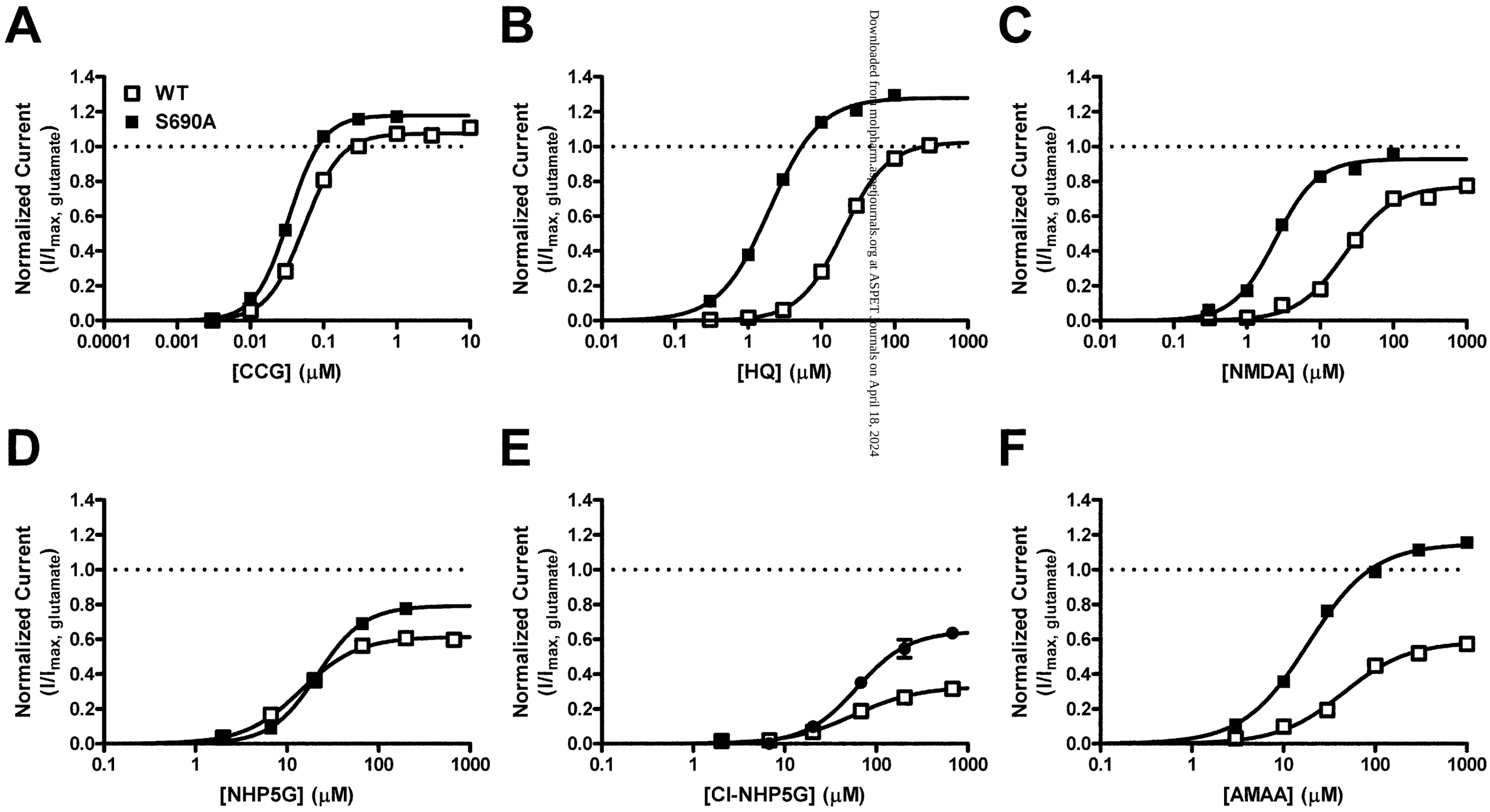

Figure 11

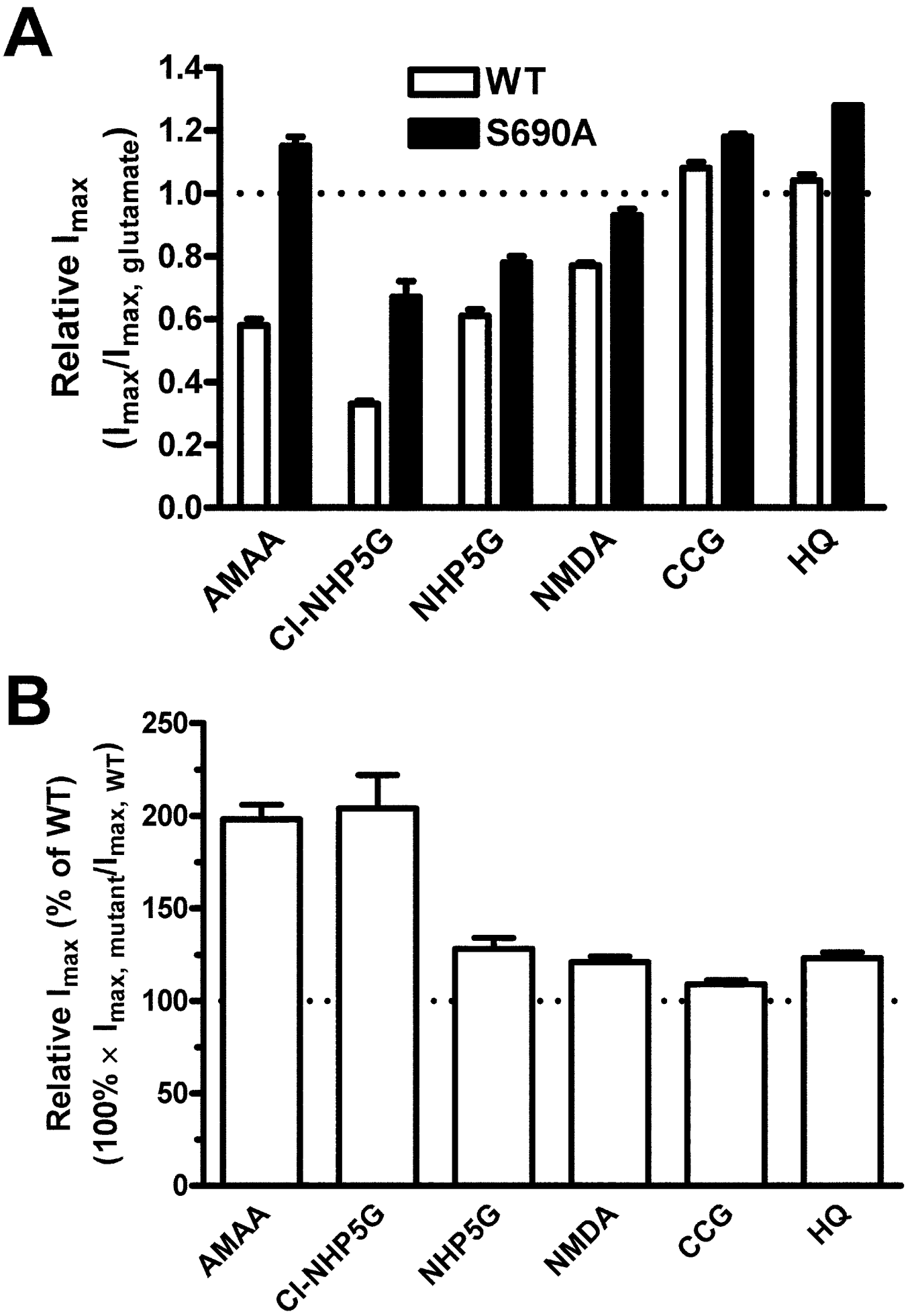
A
WT
S690A
Relative I_{max}
($I_{max}/I_{max, glutamate}$)
1.4
1.2
1.0
0.8
0.6
0.4
0.2
0.0
AMAA
Cl-NHP5G
NHP5G
NMDA
CCG
HQ
B
Relative I_{max} (% of WT)
(100% × $I_{max, mutant}/I_{max, WT}$)
250
200
150
100
50
0
AMAA
Cl-NHP5G
NHP5G
NMDA
CCG
HQ

Figure 12

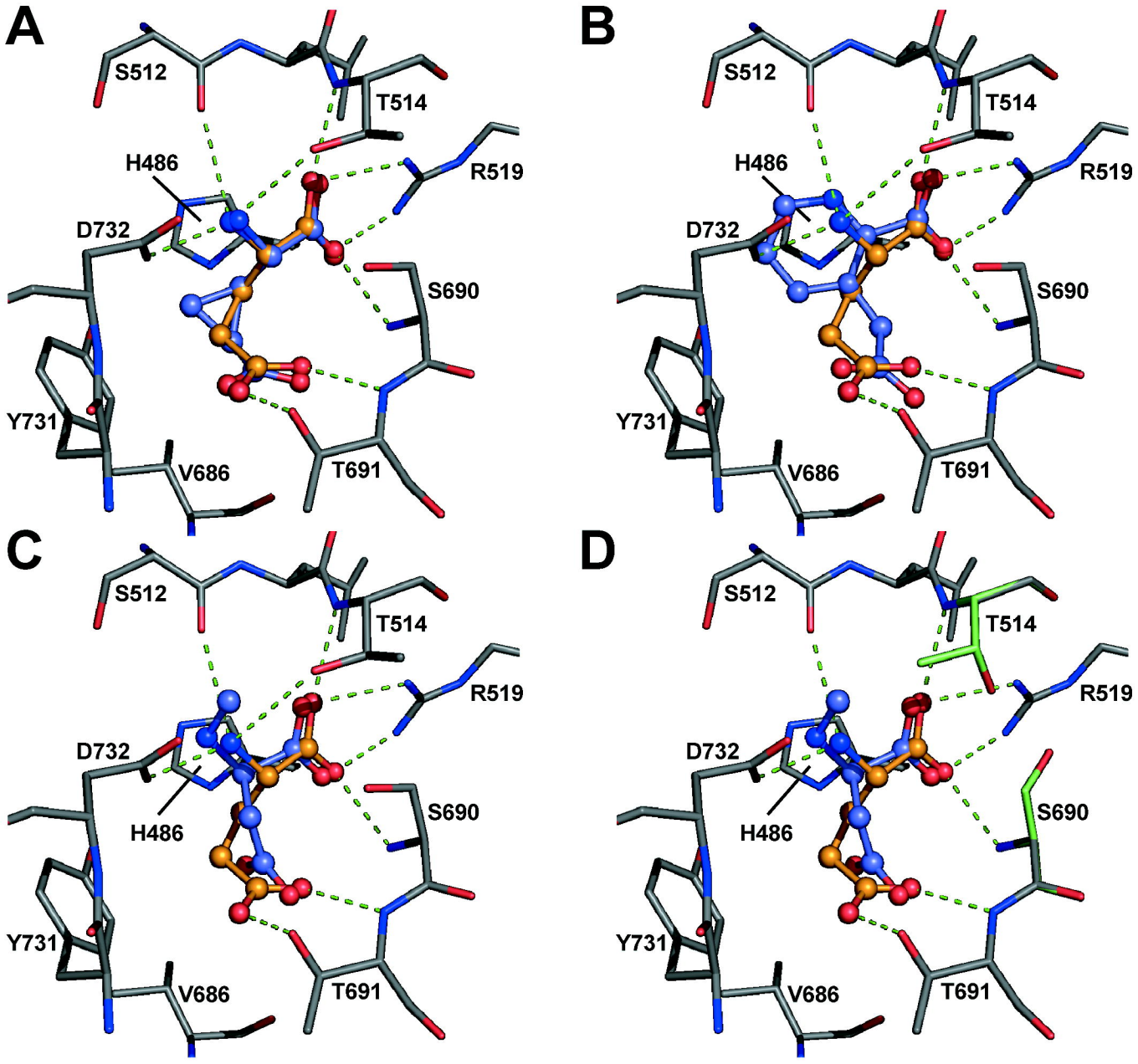
A
S512
T514
H486
R519
D732
S690
Y731
V686
T691
B
S512
T514
H486
R519
D732
S690
Y731
V686
T691
C
S512
T514
R519
D732
H486
S690
Y731
V686
T691
D
S512
T514
R519
D732
H486
S690
Y731
V686
T691

Ligand-Induced Conformational Changes of S688 in NR1. The interpretation of the observed results at NR2B(S690A) prompted a closer inspection of the published NR1 structures (Furukawa and Gouaux, 2003; Inanobe et al., 2005). For all complexes of NR1-S1S2 containing an agonist with high relative efficacy (i.e. glycine, D-serine, and 1-aminocyclopropane-1-carboxylic acid (ACPC)) there is a hydrogen bonding network from S688 to T518 (S690 to T514 in NR2B), either through one water molecule or via the hydroxyl group of D-serine (Fig. 1A, B and C). In the complexes with partial agonists, this bonding pattern is absent. Thus, in the structure of NR1-S1S2 complexed with D-cycloserine (Fig. 1D), S688 hydrogen bonds to the ligand heterocycle instead of the water bound by T518. In the case of NR1-S1S2 complexed with 1-aminocyclobutane-1-carboxylic acid (ACBC) (Fig. 1E), S688 is flipped to an alternative position. We speculate that for NR1, agonist potency and efficacy may be influenced by the binding patterns of S688 and T518. It seems likely that some flexibility is present in this region and the exact position of this residue is determined by the structure of the complexed ligand combined with the nature of the surrounding water architecture. In this respect, the crystal structures presumably display the most abundant and low-energy conformational states of these residues.

References

Furukawa H and Gouaux E (2003) Mechanisms of Activation, Inhibition and Specificity: Crystal Structures of the NMDA Receptor NR1 Ligand-Binding Core. *EMBO J* **22**:2873-2885.

Inanobe A, Furukawa H and Gouaux E (2005) Mechanism of Partial Agonist Action at the NR1 Subunit of NMDA Receptors. *Neuron* **47**:71-84.

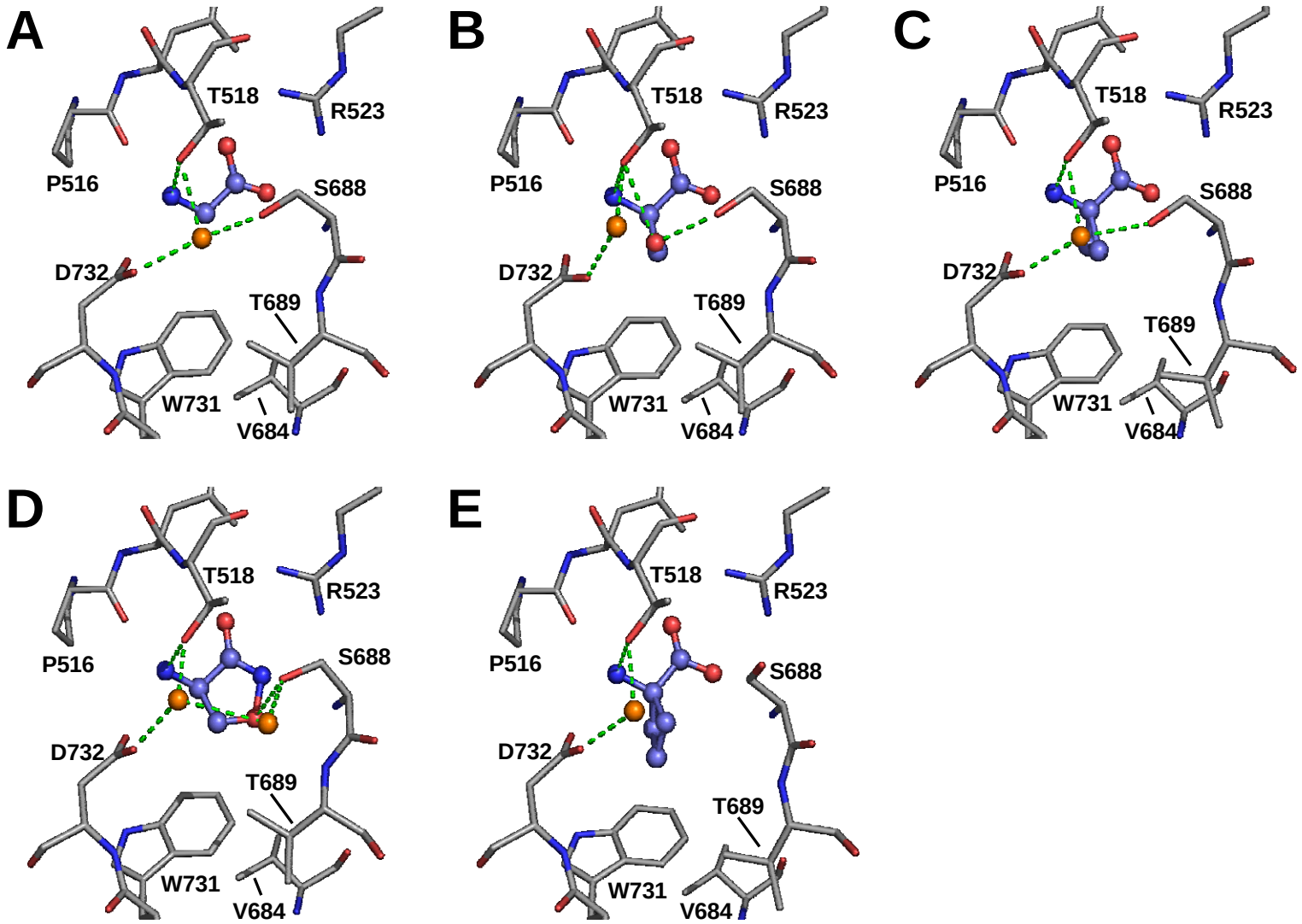

Figure 1. Key interactions upon binding of glycine (A), D-serine (B), ACPC (C), D-cycloserine (D), and ACBC (E). Shown here are interactions between the agonist, water, and residues T518, S688, and D732 in the ligand binding pocket of NR1. Notice that S688 has flipped to an alternative position upon binding of ACBC. Potential hydrogen bonds are displayed as green dotted lines. Carbon (grey), nitrogen (blue), and oxygen (red) atoms of the binding pocket are presented as sticks. Atoms of water (orange) and ligands are presented as ball and stick. Carbon atoms of the ligands are colored in marine. F484 is omitted for clarity. This figure is based on structures deposited in the Protein Data Bank with accession codes 1PB7 (glycine), 1PB8 (D-serine), 1Y20 (ACPC), 1PB9 (D-cycloserine), and 1Y1Z (ACBC). The figure was prepared using PyMol software (DeLano Scientific, San Francisco, CA).